EPJ manuscript No.
(will be inserted by the editor)

Spectroscopy of ^{17}C and $(sd)^3$ structures in heavy carbon isotopes

H.G. Bohlen[1], R. Kalpakchieva[2,3], W. von Oertzen[1,4], T.N. Massey[5], A.A. Ogloblin[6], G. de Angelis[7], M. Milin[8], Ch. Schulz[1], Tz. Kokalova[1], and C. Wheldon[1]

[1] Hahn-Meitner-Institut Berlin, Glienicker Strasse 100, D-14109 Berlin, Germany
[2] Flerov Laboratory of Nuclear Reactions, JINR, RU-141980 Dubna, Russia
[3] Institute for Nuclear Research and Nuclear Energy, BAS, Blvd. Tsarigradsko Shosse 72, BG-1784 Sofia, Bulgaria
[4] Freie Universität Berlin, Fachbereich Physik, Arnimallee 14, D-14195 Berlin, Germany
[5] Department of Physics and Astronomy, Ohio University, Athens, Ohio 45701-2979, USA
[6] IGNP, RCC Kurchatov Institute, Kurchatov Square 1, RU-123182 Moscow, Russia
[7] INFN, Laboratori Nazionali di Legnaro, I-35020 Legnaro, Italy
[8] Ruđer Bošković Institute, Bijenicka 54, HR-10002 Zagreb, Croatia

February 20, 2007

Abstract. The structure of ^{17}C has been investigated using the three-neutron transfer reaction (^{12}C,^{9}C) on a ^{14}C target at 231 MeV incident energy, the reaction Q-value is Q_0 = -46.930 MeV. Eleven new states up to 16.3 MeV excitation energy were identified. The same reaction has also been used on a ^{12}C target (Q_0 = -38.787 MeV), and excited states in ^{15}C up to 19 MeV were observed. In ^{17}C the three transferred neutrons populate $(sd)^3$ configurations on the ^{14}C core. The comparison of levels populated by the (^{12}C,^{9}C) reaction in ^{17}C, ^{16}C and ^{15}C reveals a strong similarity of their properties. This concerns especially nine states in each of the three carbon isotopes, which show practically the same excitation energies except a constant mean shift of +5.82 MeV for ^{16}C and +6.65 MeV for ^{15}C with respect to ^{17}C. The triples of states from the three isotopes, which correspond to each other, have also similar widths and cross section ratios. It is concluded that the same $(sd)^3$ structures are populated in the three carbon isotopes. The observed levels of ^{17}C are also compared to the levels of ^{19}O with known assignments and to shell-model calculations, and their decay properties are discussed.

PACS. 2 1.10.Hw, 21.10.Pc, 25.70.Hi, 27.20.+n

1 Introduction

The ground state properties of neutron-rich carbon isotopes (A≥15) have been investigated by many authors in radioactive-beam experiments using single-neutron removal reactions in order to obtain information about the halo structure from the momentum distributions (see *e.g.* refs. [1–5]). Spin-parities of the ground states have been obtained using the dependence of the momentum distributions and removal cross sections on the single-particle bound state properties of the removed neutron. This method has been further refined by measuring, after neutron removal, also partial cross sections and branching ratios of γ-transitions in the residual nucleus in coincidence [6,7]. Corresponding theoretical investigations of ground state properties have been performed by Ridikas *et al.* [8], Sagawa, Suzuki and Hagino [9,10], and Descouvemont [11] (see also refs. therein). Most of the interpretations of the single-neutron removal data, *i.e.* refs. [6,7], are based on neutron wave functions from shell model (SM) calculations with interactions from Warburton and Brown [12] or from Millener-Kurath [13].

For ^{17}C the mass excess and a single particle-stable excited state at 295 ±10 keV have been measured in 1977 by Nolen *et al.* [14] and later also by Fifield *et al.* [15] using in both cases the ^{48}Ca(^{18}O,^{17}C)^{49}Ti reaction. But in this reaction only excited states below the neutron threshold of ^{17}C at 0.729 MeV can be observed. These authors expected from systematic trends for the spin-parity of the ground state possible values of $1/2^+$, $3/2^+$ or $5/2^+$, because the corresponding lowest-lying states were estimated to be almost degenerate in ^{17}C [14]. A unique assignment of the ground state could be achieved later by exclusion of two of the three values: On the one hand Warburton and Millener [16] showed in the analysis of the feeding ratios of γ-transitions in ^{17}N after β^- decay of ^{17}C [17], that a $5/2^+$ assignment "is highly disfavoured independent of any model", and this assignment should be excluded. A decision in favour of one of the remaining options could not be made from this analysis, although a preference for

Correspondence to: bohlen@hmi.de

$3/2^+$ was found from the value of the half-life (experimental value: 202±30 ms [18]). On the other hand, g-factor measurements for the ^{17}C ground state by H. Ogawa *et al.* [19] excluded definitely the assignment $1/2^+$, because the measured g-factor is almost six times smaller than the value predicted for $1/2^+$ by reliable theoretical calculations [10,19], whereas it agrees well for the $3/2^+$ and $5/2^+$ assignments (both values are almost equal). Since $5/2^+$ is excluded by the analysis of the β^- decay data and $3/2^+$ agrees well in all cases, only the latter value remains for the spin-parity of the ground state. This assignment is also found as the optimum value in most of the analyses of the single-neutron removal measurements [4,6,7].

Recently Stanoiu *et al.* [20] identified in the in-beam γ-spectroscopy of ^{17}C two γ-lines at 207(15) keV and 329(5) keV. These results have been confirmed by Elekes *et al.* [21], who found 210(4) keV and 331(6) keV in the inelastic scattering p(^{17}C,^{17}C')p. They showed that these γ-lines are uncorrelated and belong to transitions from two different excited states to the ground state, the γ-transition from the 0.33 MeV state being much stronger. This could be well explained using main configurations of $[\nu(1d5/2)^3]$ $5/2^+$ for the former and $[\nu(1d5/2)^2 \otimes 2s1/2]$ $1/2^+$ for the latter state. The results from the three-nucleon transfer reaction ^{48}Ca(^{18}O, ^{17}C)^{49}Ti$_{g.s.}$ [14,15] can also be understood with these assignments consistently. In this reaction the largest cross section is expected for the $5/2^+$ state, in good agreement with the observations. The cross section for the ground state ($3/2^+$) is much weaker, and a state at about 0.2 MeV ($1/2^+$) was not observed, the cross section for the $1/2^+$ state is obviously too small.

Above the neutron threshold (0.729 MeV) three states of ^{17}C could be observed in the β-decay of ^{17}B using $\beta-$ neutron coincidences and the neutron time-of-flight [22]. Their excitation energies are 3.82(5) MeV, 2.64(2) MeV and (2.25(2)) MeV, the latter value was given only tentatively (another weak structure at 1.18 MeV excitation energy is most probably part of the background, when a more realistic shape is used for the background). According to the measured log*ft*-values these states are assumed to have odd parity, but assignments have not been made by the authors. SM-calculations for these states are discussed at the end of sect. 4.2.

It is expected, that most levels in the low excitation energy range have a three-neutron (sd)^3 configuration coupled to the core of the ^{14}C ground state with a closed neutron (1p) shell. These structures are characterized as neutron 3-particle - 0-hole (3p-0h) states with even parity. A direct three-neutron transfer on ^{14}C can easily populate these configurations.

Neutron (1p-1h) excitations of the ^{14}C core will lead to neutron (4p-1h) odd-parity states in ^{17}C, but these can be populated only in a higher-order process starting from the ^{14}C ground state.

Structures with core excitations may be also discussed in ^{16}C for comparison. The states of ^{16}C have been studied by Balamuth *et al.* [23], Fortune *et al.* [24,25] and Sercely *et al.* [26] using the two-neutron transfer reaction ^{14}C(t,p)^{16}C. In this case core excitations of the ^{14}C core lead to (3p-1h) odd parity states. No such states could be identified in this reaction up to 5 MeV, only at 6.11 MeV a state with tentative assignments (2^+, 3^-, 4^+), including an odd parity, was found. However, odd parity states were definitely identified in ^{16}C above 7 MeV in our previous measurement of the ^{13}C(^{12}C,^{9}C) reaction [27]. The (3p-1h) configurations are populated, because the ^{13}C target nucleus serves as a core with a built-in neutron 1p1/2-hole. These structures were identified up to 10.4 MeV, and they are expected to extend also to higher excitation energies.

In ^{17}C the excitation of protons may contribute to states at excitation energies above 7 MeV, since the lowest 2^+ state of ^{14}C is located at 7.01 MeV, which has a dominant proton configuration. Apart from such proton excited configurations there should be a strong similarity between the level schemes of ^{17}C and ^{19}O concerning the (sd)^3 neutron structures. For the understanding and description of these states it is important to treat all *three* neutrons outside the closed shell cores ^{14}C and ^{16}O, respectively, as valence particles. Two of the three neutrons may couple not only to 0^+ (giving rise to the single-neutron configurations based on the lowest-lying 0^+ state of ^{16}C), but also 2^+ or 4^+ are possible, which increases the number of spin couplings and configurations tremendously. Strong configuration mixing and large deformations are expected.

The (^{12}C,^{9}C) three-neutron transfer reaction, which we have used to investigate the level structure of ^{17}C, has a very large negative Q-value, $Q_0 = -46.93$ MeV, and requires therefore relatively high incident energies. In this case both, the high projectile velocity and the large negative Q-value will lead to a suppression of higher order contributions with respect to the lowest order transitions. In the following we will refer to the direct 3n-transfer as the first order process. Significant contributions from second order processes like target particle-hole excitations in combination with the three-neutron transfer are not expected.

2 Experimental

2.1 Measurements

The measurements of the ^{14}C(^{12}C,^{9}C)^{17}C reaction have been performed at the Q3D magnetic spectrograph at ISL, Hahn-Meitner-Institut Berlin. The ^{12}C beam of 231.3 MeV incident energy was delivered by the isochron-cyclotron at ISL. The composition of the ^{14}C target has been measured using the ERDA method (Elastic Recoil Detection Analysis) to determine absolute layer thicknesses. The following values have been obtained (a systematic error of about 5-10% is estimated):
^{14}C: 384 μg/cm^2; ^{12}C: 50 μg/cm^2; ^{13}C: $\leq$1 μg/cm^2;
^{16}O: 8 μg/cm^2; other constituents (Z=11-30): $\sim$8 μg/cm^2.
Contributions in the spectrum from the ^{16}O content were negligibly small. The heavier constituents gave rise to a continuous background with a flat shape, as will be shown later. The significant ^{12}C content of the ^{14}C target required the measurement of a spectrum of the ^{12}C(^{12}C,^{9}C) reaction on a separate ^{12}C target (thickness 200 μg/cm^2)

for background subtraction. This reaction has been measured at two different magnetic field settings (fig. 1, upper and central panels) for a precise energy calibration of the focal plane. A systematic error of $\delta E_x \leq \pm 0.04$ MeV is estimated for the excitation energy scales of both, the ^{15}C and the ^{17}C spectra. The angular acceptance of the spectrograph was defined by the entrance slits for the range of scattering angles from 3.0^o to 7.0^o horizontally and $\pm 1.5^o$ vertically.

The focal plane detector determines the position by the delay-line read-out technique. The high linearity between the momentum of the particle and the position in the focal plane, which is related to the constant dispersion in the focal plane [28], is well reproduced by the actual calibration, as also in previous measurements (see *e.g.* [27, 29]. An overall energy resolution of 220 keV was obtained for the ^{12}C target, and 250 keV for the ^{14}C target due to its larger thickness. The reaction products were identified using the energy-loss (ΔE) of the particles in the gas-filled focal plane detector, the energy signal (E) from the scintillator behind it and the time-of-flight (ToF) of the particles through the spectrograph. The dependence of the time-of-flight ToF(θ) of the particle on the scattering angle θ was used to obtain the scattering angle θ_{Lab}. Partial angular distributions have been measured in this way for ^{15}C within the entrance aperture with an angular resolution of 0.3^o. This technique could not be applied for ^{17}C states, because the background in the ^{17}C spectrum arising from the ^{12}C content of the ^{14}C target was too large. The measured correlations between the momentum and θ_{Lab} have been used to optimize the resolution by performing kinematical corrections off-line. More details about the experimental method are given in [29].

2.2 Resonances, stretched configurations

In the analysis of the experimental spectra the states above the neutron thresholds (S_n= 1.218 MeV for ^{15}C and S_n= 0.729 MeV for ^{17}C) are described as single Breit-Wigner resonances:

$$\sigma(E_{dec}) \sim \frac{\Gamma_\ell(E_{dec})\ \Gamma_\ell(E_R)}{[E_{dec} - E_R - \Delta_\ell(E_{dec})]^2 + [\frac{1}{2}\Gamma_\ell(E_{dec})]^2} \quad (1)$$

The width $\Gamma_\ell(E_{dec})$ and the shift function $\Delta_\ell(E_{dec})$ are calculated according to eqs. (2) and (3) using the decay energy $E_{dec} = E_x - S_n$ as independent variable and assuming a decay to the ground state of the daughter nucleus. If the decay leads to an *excited* state at $E_{x,f}$ in the final nucleus, the decay energy E_{dec} is reduced by this amount (this is discussed in sect. 4.5).

$$\Gamma_\ell(E_{dec}) = \Gamma_R \times P_\ell(E_{dec})/P_\ell(E_R) \quad (2)$$

$$\Delta_\ell(E_{dec}) = [Q_\ell(E_{dec}) - Q_\ell(E_R]/P_\ell(E_R) \times \Gamma_R/2 \quad (3)$$

The functions $P_\ell(E_{dec})$ (penetrability) and $Q_\ell(E_{dec})$ are defined by Coulomb functions in the usual way [30]. They depend on the decay angular momentum ℓ. A channel radius of 6 fm is used in this analysis. The dependence of the width $\Gamma_\ell(E_{dec})$ on the decay energy and ℓ-value is formulated in eq. (2) in a way, which guarantees, that the fitted experimental width parameter Γ_R is obtained exactly at $E_{dec} = E_R$ independent of the fact, whether the *maximum* of the calculated distribution is observed at E_R or not. This has been achieved by a suitable choice of the boundary condition B_ℓ [30] for the shift function $\Delta_\ell(E_{dec})$, that $\Delta_\ell(E_{dec})$ vanishes at $E_{dec} = E_R$ in eq. (3). In this formulation the extracted experimental values of *the resonance energy E_R and the width Γ_R are not dependent on the assumed decay ℓ-value*, which is especially important for broad resonances not far from the threshold.

In this work the term *stretched configuration* is used at different places to characterize a special type of coupling of several angular momenta, e. g., SM-orbits of two or three nucleons. This term denotes configurations, where the angular momenta of the active nucleons in *given* SM-orbits couple to the *maximum* angular momentum allowed by the Pauli principle. For example, the stretched configuration of three neutrons in a $(1d5/2)^3$ coupling has an angular momentum of $9/2^+$. Stretched configurations are usually populated with the largest cross sections in heavy-ion induced transfer reactions, when the reaction Q-value of the considered two-body reaction channel is very large, either positive or negative, and/or the height of the Coulomb barrier changes strongly. Then the grazing angular momenta of the entrance and exit channels, $L_{gr,i}$ and $L_{gr,f}$, respectively, are very different. Optimum reaction conditions to obtain large cross sections require in this case large angular momentum transfers ℓ_{tr}. Stretched configurations can "bridge" the gap between $L_{gr,i}$ and $L_{gr,f}$ in the best way. These dynamical angular-momentum *matching* conditions and corresponding rules are discussed in detail by Brink [31]. We will come back to this point in sect. 4.

2.3 Background

Fig. 1 shows typical spectra of the (^{12}C,^{9}C) reaction on ^{12}C. Besides the states of ^{15}C there appear in the high excitation energy region broad distributions, which correspond to three-body backgrounds with the particles ^{9}C + n + ^{14}C* in the exit channel, from which only ^{9}C is detected. While the upper and lower panels of fig. 1 show only part of these distributions, they are observed in full extention in the central panel.

These three-body contributions arise from the sequential decay of highly excited ^{10}C*, which is formed in the 2n-transfer reaction ^{12}C(^{12}C,^{10}C*)^{14}C*, into $^9C_{g.s.}$ + n. The decay strength distribution in ^{10}C for the decay into $^9C_{g.s.}$ + n is described by a Gaussian positioned at excitation energies in ^{10}C above the neutron threshold, $S_n(^{10}C)$ = 21.286 MeV. The corresponding parameters are fixed by the condition that the result should fit the shape of the observed background in the spectra. In the actual case the position of the Gaussian is located just 0.9 MeV above the neutron threshold of ^{10}C and the width is 0.7 MeV (FWHM). The very high-lying neutron threshold limits strongly the decay into the neutron channel, because other decay channels (p-, 2p-, α-, ^{3}He-emission) are open at

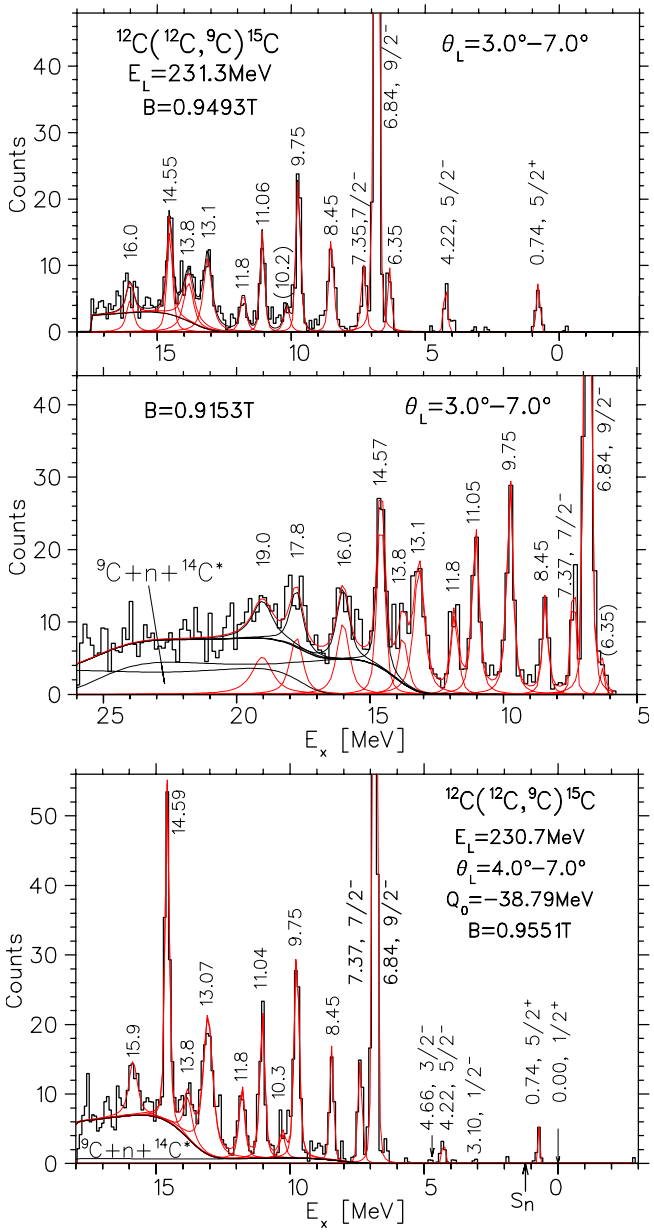

Fig. 1. (Color online) Upper and central panels: Spectra of the three-neutron transfer reaction ^{12}C(^{12}C,^{9}C)^{15}C at E_{Lab} = 231 MeV and two different magnetic field settings (upper panel: B = 0.9493 T, central panel: B = 0.9153 T). Lower panel: Spectrum of ^{15}C measured at a field setting of 0.9551 T in a previous experiment for the spectroscopy of ^{16}C [27] in a smaller angular range from 4^o to 7^o. The excitation energy scales are 120 keV/channel for the upper and lower panels, and 180 keV/channel for the central panel. Numbers are excitation energies in MeV.

much lower excitation energies. Therefore the observed three-body distributions with ^{9}C as detected particle are relatively weak.

Such distributions exist in principle in combination with all the states of the recoil nucleus ^{14}C* populated in the 2n-transfer reaction, but only the combination with the strongest states of ^{14}C are important in the analysis. These are the 3^- state at 6.73 MeV with a neutron $(1d5/2)^1(1p1/2)^{-1}$ configuration, and the 4^+ state at 10.74 MeV with a stretched neutron $(1d5/2)^2(1p1/2)^{-2}$ configuration with respect to the ^{14}C ground state (see fig. 1, upper panel, of ref. [27], and ref. [32]). The two resulting three-body distributions can be seen in the central panel of fig. 1, they rise at about 13 MeV and 17 MeV excitation energy, respectively. For the spectra measured at the higher field settings the distribution in combination with the 10.74 MeV state did not fall into the momentum acceptance of the focal plane.

In the analysis of all the spectra obtained in the (^{12}C, ^{9}C) reaction on the different targets ^{12}C, ^{13}C and ^{14}C the same neutron-decay strength distribution of ^{10}C* has been used, as described above. For the ^{13}C and ^{14}C targets the three-body distributions had to be calculated in combination with the following states of the recoil nuclei to fit the spectra of ^{16}C and ^{17}C: the state at 0.74 MeV ($5/2^+$) in ^{15}C* and the state at 4.14 MeV (4^+) in ^{16}C*, respectively. There exist also higher-lying states with large cross sections in the spectra of the recoil nuclei, but the corresponding three-body distributions do not fall into the momentum acceptance of the focal plane for the spectra of ^{16}C and ^{17}C, respectively. The three-body distributions calculated in this way have been used to describe the corresponding background observed in the spectra of ^{16}C [27]) and ^{17}C (sect. 3.2). More details about the method can be found in [29] and refs. therein.

3 Results

Since the ^{14}C target contained about 11% ^{12}C, a spectrum of the ^{12}C(^{12}C,^{9}C)^{15}C reaction was needed for background subtraction in the ^{17}C spectrum. This spectrum and also the ^{15}C spectra measured for the energy calibration and another one obtained in a previous measurement [27] are analyzed in detail, especially in the excitation energy region above 6 MeV. The results from this analysis are presented at first, before the results for ^{17}C are shown.

3.1 The ^{12}C(^{12}C,^{9}C)^{15}C reaction

The spectra of the ^{12}C(^{12}C,^{9}C)^{15}C reaction from the actual measurement are shown in the upper and central panels of fig. 1 for two different magnetic field settings. The results of the analysis are given in table 1. This reaction was measured already previously in the spectroscopic study of ^{16}C [27] for calibration and background subtraction purposes, and this spectrum is shown in the lower panel of fig. 1. The magnetic field setting was very similar as for the higher field of the present measurement (fig. 1, upper panel). In ref. [27] only the excitation energies of ^{15}C were given, and only the assignment of the doublet at 6.84 MeV / 7.37 MeV was discussed. Now the widths and cross sections are also given in table 1 (columns 4 and 5) for all the eleven states between 6.84 MeV and

Table 1. States of ^{15}C observed in the three-neutron stripping reaction ^{12}C(^{12}C,^{9}C)^{15}C at 231 MeV for two different angular ranges: $3^o - 7^o$ (columns 1 - 3), and $4^o - 7^o$ (columns 4, 5). The following entries are shown: excitation energies E_x, widths of resonances Γ_R, cross sections $d\sigma/d\Omega$ in the center-of-mass system for the present measurement, widths and cross sections for the previous measurement [27], assignments deduced from the (^{12}C,^{9}C) reaction (see also Table 4 and sects. 4.4, 4.5) and, for comparison, assignments from the literature.

^{12}C(^{12}C,^{9}C)^{15}C, E_L=231 MeV							^{9}Be(^{7}Li,p)	^{13}C(t,p)	^{14}C(d,p)
θ_L=3^o-7^o			θ_L=4^o-7^o [27]		J^π	[34]	[35]	[36]	[37,38]
E_x, J^π [MeV]	Γ_R [MeV]	$d\sigma/d\Omega$ [$\mu b/sr$]	Γ_R [MeV]	$d\sigma/d\Omega$ [$\mu b/sr$]	[27] and this work	E_x [MeV]	J^π assignments		
0.00						g.s.		$1/2^+$	$1/2^+$
0.74		0.19(9)		0.05(2)		0.740		$5/2^+$	$5/2^+$
4.22		0.17(5)		0.04(2)		4.220(3)	(5/2, 7/2)	$5/2^-$	$(7/2^+)$
6.35(2)	<0.01	0.23(7)	–	–		6.358(6)	(5/2)		$(7/2, 9/2)^+$
6.84(2)	0.02(1)	3.8(7)	0.02(1)	2.40(15)	$9/2^-$	6.841(4)	(11/2 , 13/2)	$(7/2, 9/2)^-$	
7.37(5)	0.03(2)	0.28(5)	0.05(3)	0.31(5)	$7/2^-$	7.352(6)	(9/2 , 11/2)	$(9/2, 7/2)^-$	
8.45(3)	0.08(4)	0.46(9)	0.03(2)	0.27(5)	$(3/2^+ - 7/2^+)$	8.47(15)	(9/2 - 13/2)		
9.75(2)	0.08(5)	0.90(5)	0.08(5)	0.79(8)	$(9/2^+)$	9.79(2)	(9/2 - 15/2)		
10.2(1)	0.15(12)	0.2(1)	0.15(8)	0.14(4)		10.25(2)	(5/2 - 9/2)		
11.05(3)	0.12(5)	0.66(6)	0.10(5)	0.55(7)	$(5/2^+ - 9/2^+)$	11.02(3)	(11/2 - 19/2)		
11.8(8)	0.16(8)	0.33(5)	0.20(7)	0.37(6)		11.83(2)	(≥13/2)		
13.1(1)	0.30(8)	0.94(9)	0.30(6)	1.00(9)	$(5/2^+)$				
13.8(2)	0.3(2)	0.38(5)	0.3(2)	0.31(6)					
14.57(5)	0.14(5)	0.80(7)	0.08(4)	1.04(9)	$(11/2^+)$				
16.0(2)	0.3(1)	0.40(5)	0.3(1)	0.38(6)					
17.8(2)	0.4(2)	0.51(8)							
19.0(2)	0.8(5)	0.56(4)							

15.9 MeV. In the present experiment the measured angular range is extended to smaller scattering angles until 3^o (fig. 1, upper panel). The cross sections are therefore slightly different as compared to the ones of the previous measurement (columns 3 and 5 in table 1).

The measurement of the ^{12}C(^{12}C,^{9}C) reaction has also been performed at exactly the same magnetic field setting needed for the spectroscopy of ^{17}C states (B= 0.9153 T). The corresponding spectrum is shown in the central panel of fig. 1. At this lower field we find two more resonances: at 17.8(2) MeV and 19.0(2) MeV. With these measurements at the two field settings the ^{15}C spectra cover a range of excitation energies from the ground state up to 26 MeV (fig. 1).

At the higher field settings (fig. 1, upper and lower panels) the spectra are free from contamination lines from oxygen, which indicates, that the oxygen content in the ^{12}C targets is very small. Consequently, this is also true for the measurements at the lower field (fig. 1, central panel) using the same ^{12}C target. Concerning contributions from the ^{13}C content (1.1 %) of natural carbon we can say, that the strongest line of ^{16}C, the 4^+ state at 4.14 MeV [27], is observed in fig. 1, upper and lower panels, only as one single count on the right side of the peak at 4.22 MeV, therefore all other states of ^{16}C do not contribute to the actual ^{15}C spectra.

States of ^{15}C were known from other reactions [34–38] up to 11.825(20) MeV excitation energy. The energies of the states, which we observed up to this value, agree with the values from the literature within ±30 keV. As discussed in [27] the strongest line of ^{15}C in fig. 1 at 6.84 MeV excitation energy corresponds to the $\frac{9}{2}^-$ state with stretched $[(1d\frac{5}{2})^2_{4^+}(1p\frac{1}{2})^{-1}]_{9/2^-}$ (2p-1h) neutron configuration. The coupling partner $\frac{7}{2}^-$ at 7.37 MeV with anti-parallel spin coupling of the $1p\frac{1}{2}$-hole is populated a factor of about ten more weakly.

In the analysis of the spectra the Breit-Wigner line shape was folded with the experimental resolution (220 keV for the ^{12}C target). The excitation energies displayed in the three spectra of fig. 1 were obtained in individual fits of each spectrum. Since they show small differences, only mean values are given in column 1 of table 1. These can be compared to values from the literature [34] given in column 7. A small peak at 12.6 MeV cited in our previous measurement [27] could not be identified in the present data, probably because it is very weak and positioned on the tail of the 13.1 MeV state. However, two other weak states, known from ref. [34] at 6.35 MeV $(5/2^+ - 9/2^+)$ and 10.2 MeV (5/2 - 9/2), could be confirmed.

The widths obtained in both measurements (table 1) agree well within the errors. Values of Γ_R are known from the literature [34] for most of the states up to 11.82 MeV, and our values are in agreement up to 8.47 MeV, whereas we find larger widths for the states above.

Although the angular acceptance of the present measurement includes a range of smaller scattering angles (the lower limit is at 3^o) as compared to the previous run (4^o), most of the cross sections agree within the error bars. However, in a few cases differences are observed. For the states at 0.74 MeV, 4.22 MeV, 6.35 MeV, 6.84 MeV the cross sec-

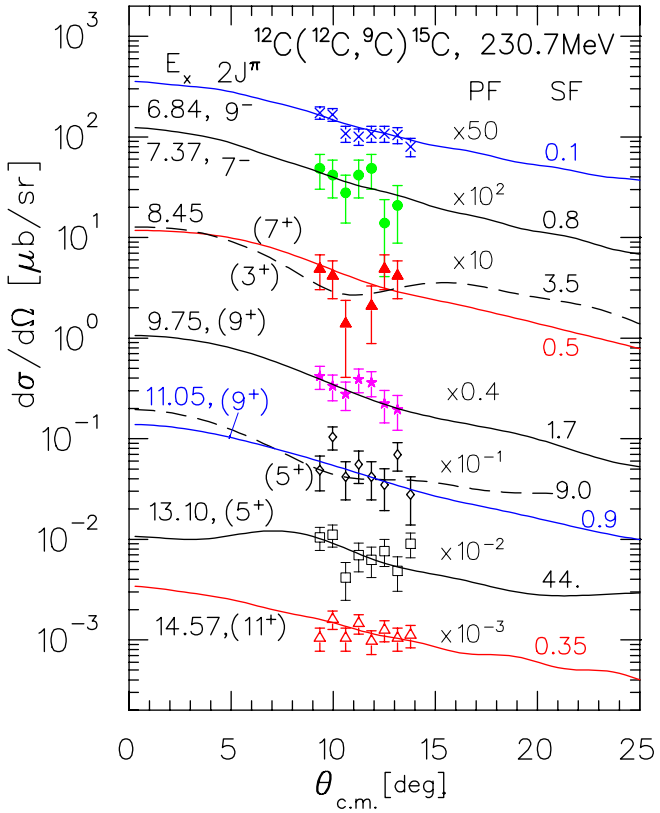

Fig. 2. (Color online) Partial angular distributions of states populated in the ^{12}C(^{12}C,^{9}C)^{15}C reaction at 230.7 MeV. The curves correspond to coupled channel calculations using the code Fresco [33], which are discussed in sect. 4.4. Excitation energies (in MeV), spins (multiplied by two) and parities, plot factors PF used for the plot of the angular distributions on a common scale and strength factors SF to normalize the calculations to the data are given for each state.

tions from the previous run are significantly lower than the ones obtained in the actual measurement, which indicates a rise of the angular distribution to forward angles.

Partial angular distributions have been obtained for the seven excited states of ^{15}C at 6.84 MeV, 7.37 MeV, 8.45 MeV, 9.75 MeV, 11.05 MeV, 13.10 MeV and 14.57 MeV from the time-of-flight to scattering-angle correlation (see sect. 2.1). They are shown in fig. 2, and the analysis is discussed in comparison to the results of ^{17}C in sect. 4.4.

3.2 The ^{14}C(^{12}C,^{9}C)^{17}C reaction

In fig. 3 the upper panel shows a spectrum of the ^{14}C(^{12}C, ^{9}C)^{17}C reaction after background subtraction, and in the central panel the full spectrum is shown together with a background spectrum resulting from the ^{12}C content (11%) in the target. The latter spectrum was measured at unchanged conditions, which were set for the spectroscopy of ^{17}C on the ^{14}C target. This concerns the magnetic field settings, kinematical corrections and angular acceptances. The spectrum is shown in the lower panel.

In the central panel of fig. 3 the very strong contamination line from the excited state of ^{15}C at $E_x = 6.84$ MeV can be seen, according to the energy calibration, at about 200 keV above the expected position of the ^{17}C ground state. However, a peak of the ^{17}C ground state could not be identified, first of all, because the tail of the strong ^{15}C state covers this area, and also, because another continuous background exists in the full measured excitation energy range of the spectrum (see below). At the high-energy tail of the strong ^{15}C state an additional line has to be inserted at a position of 0.31(4) MeV to fit this region correctly. This is in agreement with recent results obtained by Stanoiu *et al.* [20] and Elekes *et al.* [21] from in-beam γ-spectroscopy, which show a γ-transition at 331(6) keV in ^{17}C, whereas two results from transfer reactions to bound states of ^{17}C show slightly lower values around 295(20) keV [14,15]. The next higher-lying peak is a small contamination line from the ^{15}C excited state at 7.37 MeV, which is well separated from the strong state at 6.84 MeV. Both states are the members of the $7/2^-$, $9/2^-$ doublet of ^{15}C with a neutron $(4^+ \otimes 1/2^-)$ (2p-1h) structure, which has been discussed already in the previous section.

Above the 7.37 MeV state of ^{15}C the background *from the ^{12}C content in the target* decreases almost to zero and stays low for almost 1 MeV, before the 8.45 MeV state becomes visible (see lower panel). However, in the central panel, this minimum is filled by another background contribution, and such a situation is observed also at several other places in the spectrum. To fit the ^{17}C spectrum in the full excitation energy range it was necessary to introduce in addition a flat linear background indicated by (2) in fig. 3. The minima in the counting rate of the ^{17}C spectrum (central panel) at excitation energies between (i) 1.0 MeV and 1.8 MeV, (ii) 2.3 MeV and 2.8 MeV and (iii) 3.6 MeV and 4.0 MeV receive only very small contributions from the ^{12}C background, therefore other contaminations in the target are responsible for the counts observed here. Since the target has some content from Z≥11 elements, we assume, that these produce a flat and smooth background, which is approximated by the shown line. This flat shape can be expected due to the very different kinematical energy dependence of the reactions on these heavier elements as compared to ^{14}C. The normalization of this background is obtained from the regions (i) - (iii) mentioned above. As a consequence also the normalization of the background from the ^{12}C contamination is determined, especially through the ^{15}C states at 6.84 MeV, 8.45 MeV, 11.05 MeV and 11.8 MeV and at high excitation energies.

Similar to the ^{12}C(^{12}C,^{9}C)^{15}C reaction we observe in the ^{17}C spectrum at large excitation energies a three-body distribution originating from the sequential decay of highly excited ^{10}C* ejectiles into ^{9}C$_{g.s.}$ + n. This three-body background is calculated from the reaction ^{14}C(^{12}C, ^{9}C+n)^{16}C*, where the recoil nucleus ^{16}C is excited to the 4^+ state at 4.14 MeV. This state receives by far the largest cross section in the ^{16}C spectrum [27]; states at lower excitation energies are very weakly populated or not observed. As can be seen in fig. 3 (central panel, line (3)), the three-

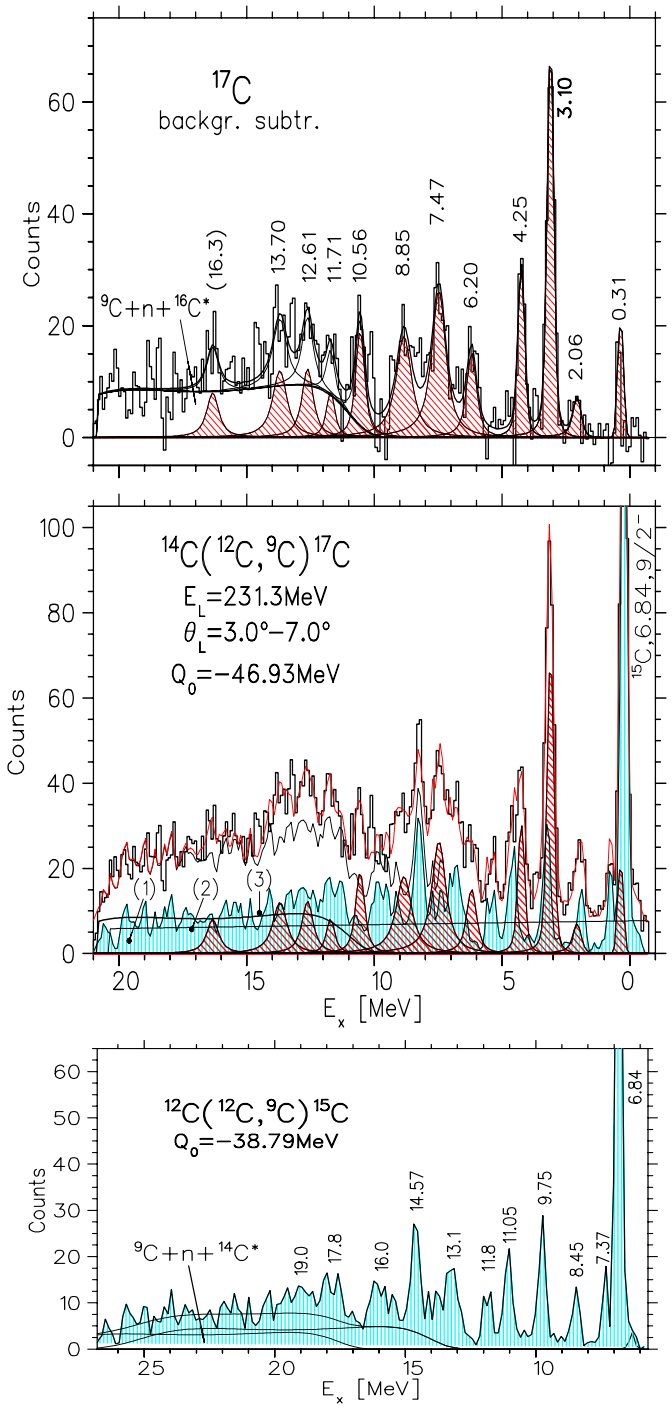

Fig. 3. (Color online) Upper panel: Spectrum of the ^{14}C(^{12}C,^{9}C)^{17}C reaction after background subtraction of contributions from target contaminations. Central panel: The spectrum as measured in the focal plane. The background (1) from the ^{12}C content in the ^{14}C target is indicated by the shaded area (colour: cyan). The strong peak on the right corresponds to the $9/2^-$ state of ^{15}C at 6.84 MeV. The linear background (2) results from target contaminations with Z $\geq$ 11. The broad distribution (3) on the left describes the fitted three-body distribution for ^{9}C + n + ^{16}C* (see sect. 2.3). States of ^{17}C are marked as downward hatched (red) areas. Lower panel: Spectrum of the ^{12}C(^{12}C,^{9}C)^{15}C reaction measured at exactly the same conditions as for ^{17}C.

Table 2. States of ^{17}C observed in the three-neutron stripping reaction ^{14}C(^{12}C,^{9}C)^{17}C at 231.3 MeV. The following entries are given from left to right: No. of the state, excitation energy, width (for a resonance), cross section in the center-of-mass system, statistical significance calculated from the full spectrum. In the lower part results from the ^{48}Ca(^{18}O,^{17}C) reaction [14, 15], the in-beam γ-ray spectroscopy in coincidence with the ^{17}C beam particles [20, 21], and from the ^{17}B β-decay [22] are shown (see SM-calculations for these states in sect. 4.2).

	^{14}C(^{12}C,^{9}C)^{17}C (this work) 231.3 MeV, $\theta_L = 3^o - 7^o$			
No.	E_x [MeV]	Γ_R [MeV]	$d\sigma/d\Omega$ [nb/sr]	signif. [σ]
1	0.00	–	$\leq$10(5)	–
2	(see lower part)			
3	0.31(4)	–	50(30)	5.0
4	2.06(5)	0.25(10)	45(25)	3.8
5	3.10(2)	0.10(5)	300(20)	19.0
6	4.25(2)	0.14(8)	140(15)	17.0
7	6.20(3)	0.35(15)	110(15)	12.0
8	7.47(3)	0.58(10)	293(30)	13.8
9	8.85(5)	0.66(20)	220(30)	9.7
10	10.56(3)	0.30(10)	130(15)	12.2
11	11.71(5)	0.30(15)	72(15)	3.5
12	12.61(3)	0.45(20)	110(15)	5.5
13	13.70(5)	0.6(2)	160(20)	4.7
14	(16.3(1))	0.5(2)	73(20)	3.2
	Other reactions:			
	(^{18}O,^{17}C) [14,15] E_x [keV]	p+^{17}C - γ [20,21] E_γ [keV]	^{17}B β-decay) [22] E_x [MeV]	
1	0.00	–	–	
2	–	210(5)	–	
3	295(20)	330(5)	–	
b1			(2.25(2))	
b2			2.64(2)	
b3			3.82(5)	

body background starts to rise at about 10 MeV excitation energy and then remains almost flat up to the end of the observed excitation energy range.

In the analysis of the full spectrum Breit-Wigner resonances were introduced above E_x= 0.73 MeV (the neutron threshold). Positions, widths and normalizations were fitted together with the normalizations of the three different background distributions. In total twelve states of ^{17}C (state no. 3 - 14 in table 2) were identified. Their excitation energies, widths, cross sections and statistical significances are given in table 2 together with the results from Nolen *et al.* [14] and Fifield *et al.* [15], which were previously obtained in the ^{48}Ca(^{18}O,^{17}C)^{49}Ti$_{gs}$ reaction, from Stanoiu *et al.* [20] and Elekes *et al.* [21], and from the ^{17}B β-decay [22]. We want to note at this place, that in our previous reports [39, 40] about ^{17}C the values of excitation energies were still preliminary and therefore slightly differ in a few cases from the ones given in this final analysis.

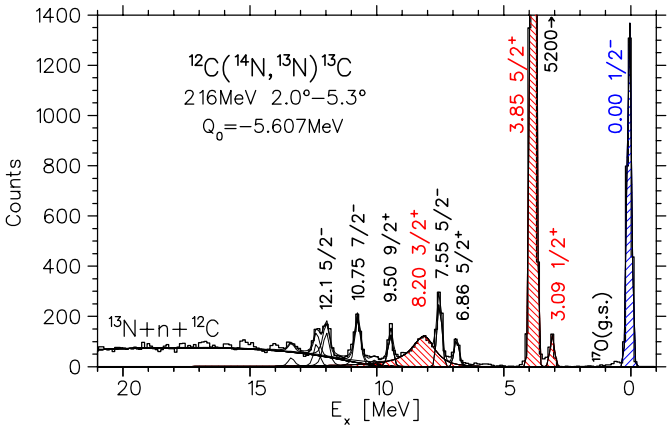

Fig. 4. (Color online) Spectrum of the ^{12}C(^{14}N,^{13}N)^{13}C reaction measured at 216 MeV incident energy. Single-particle states of ^{13}C with known spectroscopic factors of S = 0.6 - 0.7 [34, 42–45] are marked by the hatched areas. The strong difference between the cross sections of the 1d5/2 state at 3.85 MeV and the 2s1/2 state at 3.09 MeV is obvious. Indicated assignments are taken from [34, 43].

4 Discussion

In this measurement the states of ^{17}C are populated in a direct three-neutron transfer reaction on ^{14}C. It is well known, that ^{14}C has a rather inert structure in its ground state. The neutron (1p) shell is closed, only about 8% particle - hole admixtures are found in the ^{14}C(p,d) reaction [41]. Therefore it is expected, that for the lower lying states of ^{17}C the three neutrons are built into the next open orbits, ν2s1/2 and ν1d5/2. The corresponding $1/2^+$ and $5/2^+$ single-neutron states on the ^{14}C core are identified in ^{15}C as the ground state ($1/2^+$) and the first excited state at 0.740 MeV ($5/2^+$), respectively, with spectroscopic factors S close to one in both cases [37]. The 1d3/2 single-particle strength in ^{15}C is located at higher excitation energy: it is a very broad resonance in ^{15}C at 4.78(10) MeV with a width of Γ=1.74(40) MeV observed *only* in the ^{14}C(d,p) reaction [38], not in ^{9}Be(^{7}Li,p) [35] and also not in ^{13}C(t,p) [36] (we also do not observe it in the ^{12}C(^{12}C,^{9}C) reaction, see fig. 1).

In the following discussion about the structure and tentative assignments of states we will use the well known dependencies of cross sections in heavy-ion transfer reactions on spin factors, angular momentum transfers and the strength of the overlap integral between the scattering waves in the entrance and exit channels in a direct 3n-transfer. Due to the large negative Q-values, which we are dealing with in the (^{12}C,^{9}C) reaction (fig. 3), the wave number of scattering waves in the exit channel is very much decreased. Correspondingly the grazing angular momenta $L_{gr,f}$ are lowered with respect to the value in the entrance channel, $L_{gr,i}$. As a result a strong mismatch of the incoming and outgoing grazing waves occurs in the radial integral, its value and therefore the cross section is strongly reduced, especially for low-spin states. However, the mismatch is partially compensated for final states with large spins, since a large angular momentum transfer ℓ_{tr} is allowed in such cases. This ℓ-transfer helps to bridge the large difference between $L_{gr,i}$ and $L_{gr,f}$. A high angular momentum is typically obtained for stretched configurations (sect. 2.2), where the three neutron orbits are coupled to the maximum spin. The statistical spin factors of the transition amplitude are then also large and the cross section is further increased (see, e.g., [46] for more details). The transfer of neutrons into ℓ=0 final states leads to small cross sections, whereas these are much larger for the transfer into ℓ=2, j=5/2 orbits.

The spectrum of the ^{12}C(^{14}N, ^{13}N)^{13}C one-neutron transfer reaction (fig. 4) illustrates these effects. It shows the single-particle states of ^{13}C in the (sd)-shell as downward hatched areas. The tremendous difference especially between the cross sections of the $1/2^+$ and $5/2^+$ single-particle states can be explained by the matching conditions and spin factors, although the *spectroscopic factors are about the same* [34,42] for the 1p1/2, 2s1/2, 1d5/2, 1d3/2 states, respectively. Therefore we can expect for the *three-neutron transfer*, that final states with configurations, where 1 - 2 neutrons were placed into the 2s1/2 shell, are very much suppressed, but they are strong with 2 - 3 neutrons in the 1d5/2 shell.

4.1 Comparison between ^{17}C, ^{16}C and ^{15}C

As discussed in the previous section, reactions with large negative Q-values favour the population of states with stretched configurations and large spins. For example, in the ^{12}C(^{12}C, ^{9}C)^{15}C reaction [27] (Q_0= −38.79 MeV) we could assign in ^{15}C the doublet at 6.84 MeV, 7.37 MeV as $9/2^-$, $7/2^-$, respectively. The $9/2^-$ state has the stretched configuration: $[\phi_{1n}(1p1/2) \otimes \phi_{2n}([1d5/2]^2, 4^+)]9/2^-$, whereas for the $7/2^-$ state the 1p1/2 neutron is coupled anti-parallel to the 4^+ configuration. The cross section of the $9/2^-$ state is a factor of about ten larger than the one for the $7/2^-$ state (table 1, columns 3 and 5).

A very similar coupling scheme occurs in ^{16}C for the $5^-/4^-$ doublet at 8.92 MeV/9.42 MeV populated in the ^{13}C(^{12}C, ^{9}C)^{16}C reaction [27], with three neutrons transferred to the 1d5/2 shell. The stretched configuration is obtained with the following coupling:
$[\phi_{1n}(1p1/2) \otimes \phi_{3n}([1d5/2]^3, 9/2^+)\ ]\ 5^-$, and for the 4^- state the 1p1/2 neutron is coupled anti-parallel. In this case the ratio of the cross sections for the $5^-/4^-$ doublet is 3.6 [27] (fig. 5, central panel).

The ^{14}C(^{12}C,^{9}C) reaction has an even larger negative Q-value, Q_0= -46.930 MeV. According to the matching rules the strongest *low-lying* peak observed in the ^{17}C spectrum should be identified with the stretched $[(1d5/2)^3]$ $9/2^+$ configuration, without core excitations. There is only one candidate: the peak at 3.10 MeV excitation energy. The $9/2^+$ assignment for this peak is supported by further arguments as we will see later. In the following the discussion is continued with a systematic comparison of the observed levels in ^{17}C, ^{16}C and ^{15}C populated in the (^{12}C,^{9}C) three-neutron transfer reaction.

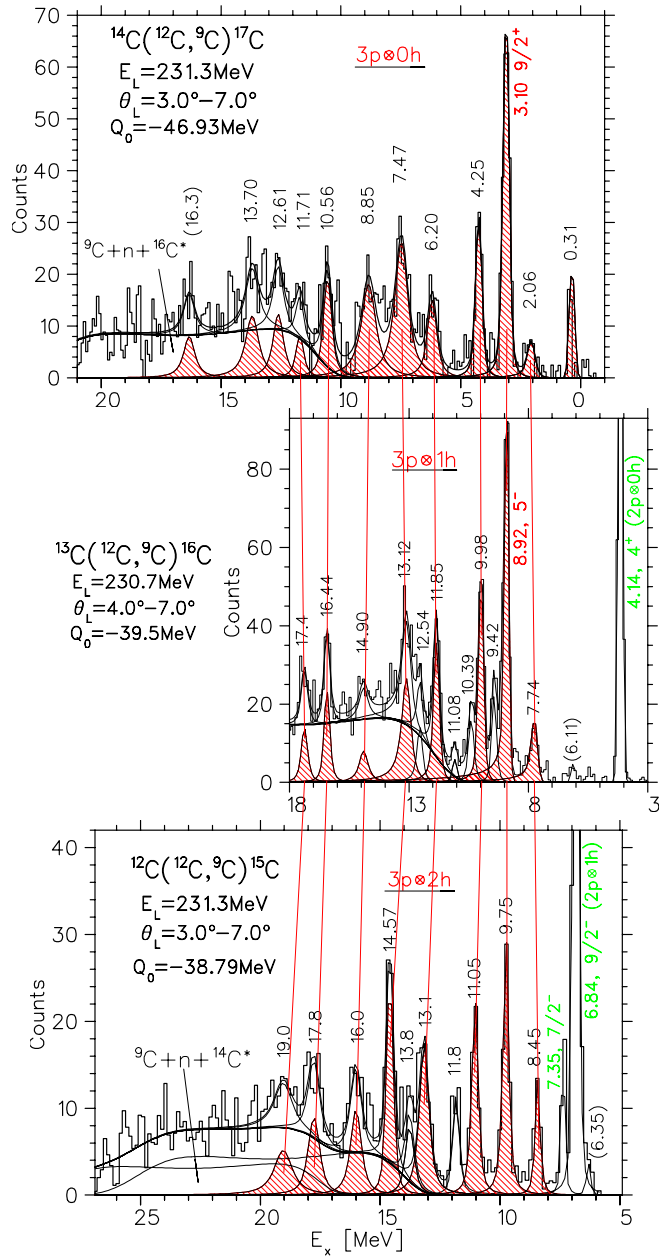

Fig. 5. (Color online) Spectra of ^{17}C (upper panel), ^{16}C (central panel) [27] and ^{15}C (lower panel) obtained in the (^{12}C,^{9}C) three-neutron transfer reactions on ^{14}C, ^{13}C and ^{12}C, respectively. The spectra of ^{16}C and ^{15}C are shifted in excitation energy by -5.82 MeV and -6.65 MeV, respectively, relative to the scale of the ^{17}C spectrum (see sects. 2.2 and 4.5 for line shapes). The lines connect the strongest *corresponding* states (table 3) of the isotopes and indicate the regular behaviour of the distances and strengths.

Most striking is the comparison of the spectra of ^{17}C and ^{16}C as shown in fig. 5, upper and central panel, when the strongest states of ^{17}C and ^{16}C with stretched (sd)^3 neutron configurations, respectively, the $9/2^+$ state in ^{17}C at 3.10 MeV and the 5^- state in ^{16}C at 8.92 MeV, are aligned to each other. The spectrum of ^{16}C is shifted for this comparison by 8.92 - 3.10 = 5.82 MeV. In total nine pairs of states up to the excitation energy of 12 MeV (for ^{17}C) are then simultaneously aligned (table 3). This comparison is limited at the high excitation energy side by the end of the ^{16}C spectrum. In fig. 5 the correspondence is indicated by the vertical lines for the eight strongest states. The excitation energies of ^{16}C, after subtraction of the constant value of 5.82 MeV, are given in table 3, line 4, as $E_x^{dif}(^{16}C)$. These values agree well with the excitation energies of ^{17}C. The maximum difference, $\delta E_x^{dif}(^{16}C)$ is not larger than -0.17 MeV/+0.23 MeV for all the pairs in this large excitation energy range.

This regular behaviour is obviously a clue for a common structure of the corresponding states. In fact, the ^{13}C core introduces for all the observed states of ^{16}C, considered here in this comparison, only a common shift of 5.82 MeV -0.17/+0.23 MeV. Then the interpretation, that this common shift is due to the neutron 1p1/2 hole in the ^{14}C core, is consistent with this observation. This must be essentially the only difference of the structure. The three-neutron configurations of the considered levels of ^{17}C and ^{16}C must be practically the same pairwise to obtain such a high degree of consistency. The 3n-wave functions modify the core structures of ^{14}C and ^{13}C obviously very little, particle-hole excitations of the cores seem to be weak. This observation confirms the weak-coupling character of the interaction between the core and the three-neutron configurations populated by the direct transfer. This character may change, when at higher excitation energies a core excitation of the proton configuration to a 2^+ state in the (1p) shell might occur in the corresponding states of ^{17}C and ^{16}C. As already discussed, we expect smaller cross sections for such second order processes, although at high excitation energies they probably become more important.

The correspondence between the states of ^{17}C and ^{16}C continues also for the widths of the resonances, at least for the pairs no. 2 - 6, the widths of both members are very similar *for these five pairs* (table 3, lines 6 - 7).

This similarity of the widths is not simply explained by the neutron thresholds in both isotopes, S_n = 0.73 MeV for ^{17}C and S_n = 4.25 MeV for ^{16}C. In the neutron decay of resonances in ^{16}C there is an about 2.3 MeV larger decay energy available as compared to ^{17}C. For example, the maximum decay energies for the members of the pair no. 3 are: (3.10 - 0.73) MeV = 2.37 MeV for ^{17}C and (8.92 - 4.25) MeV = 4.67 MeV for ^{16}C, the difference being 2.3 MeV. When in both cases the neutron decay would lead to the ground state of the daughter nucleus, and assuming the same (sd)^3 neutron configuration in both members, a larger width should be expected for the ^{16}C resonances due to the larger decay energies as compared to ^{17}C. However, this is not observed. It is necessary to take the parentage between the neutron configurations of the (sd)^3 structure of the decaying state and the (sd)^2 structure of the final state in the daughter nucleus into account. Since more information about the structure of the participating states is needed, we postpone a detailed discussion to sect. 4.5. For the remaining higher-lying pairs (no. 7 - 9)

Table 3. Comparison of excitation energies E_x, widths Γ and ratios of cross sections of nine excited states of ^{17}C and ^{16}C. The excitation energies $E_x(^{16}C)$ given in line 3 are compared to the ones of ^{17}C (line 2) by calculating the differences E_x^{dif} = E_x - 5.82 MeV and the deviations δ E_x^{dif} = E_x - 5.82 MeV - $E_x(^{17}C)$ from the ^{17}C excitation energies. The widths for the states of ^{17}C (line 6) and ^{16}C (line 7) are compared and the ratios of cross sections are given in line 8. In the lower five lines the observed excitation energies of ^{15}C are investigated in a similar way with E_x^{dif} = E_x - 6.65 MeV, and the widths $\Gamma(^{15}C)$ and ratios of cross sections $d\sigma(^{15}C)/d\sigma(^{16}C)$ are given. The excitation energies of the reference states in ^{17}C, ^{16}C and ^{15}C are marked as bold numbers.

Corresp. states, No.	1	2	3	4	5	6	7	8	9
$E_x(^{17}C)$ [MeV]	0.31	2.06	**3.10**	4.25	6.20	7.47	8.85	10.56	11.71
$E_x(^{16}C)$ [MeV]	6.11[a]	7.74	**8.92**	9.98	11.85	13.12	14.90	16.44	17.4
$E_x^{dif}(^{16}C)$=$E_x(^{16}C)$−5.82 [MeV]	0.29	1.92	3.10	4.16	6.03	7.30	9.08	10.62	11.58
$\delta E_x^{dif}(^{16}C)$=$E_x^{dif}(^{16}C)$−$E_x(^{17}C)$ [MeV]	-0.02	-0.14	±0.00	-0.09	-0.17	-0.17	+0.23	+0.06	-0.13
$\Gamma(^{17}C)$ [MeV]	–	0.25	0.10	0.14	0.35	0.58	0.66	0.30	0.30
$\Gamma(^{16}C)$ [MeV]	<0.03	0.20	≤0.10	0.12	0.22	0.40	0.30	0.15	0.20
$d\sigma(^{16}C)/d\sigma(^{17}C)$	–	2.9	2.1	2.7	3.2	1.5	0.6	1.3	1.6
$E_x(^{15}C)$ [MeV]	(6.35)	8.45	**9.75**	11.05	13.1	14.57	16.0	17.8	19.0
$E_x^{dif}(^{15}C)$=$E_x(^{15}C)$−6.65 [MeV]	(-0.30)	1.80	3.10	4.40	6.45	7.92	9.35	11.15	12.35
$\delta E_x^{dif}(^{15}C)$=$E_x^{dif}(^{15}C)$−$E_x(^{17}C)$ [MeV]	(-0.63)	-0.30	±0.00	0.15	+0.25	+0.45	+0.50	+0.59	+0.64
$\Gamma(^{15}C)$ [MeV]	–	0.08	0.10	0.10	0.30	0.13	0.30	0.50	(1.0)
$d\sigma(^{15}C)/d\sigma(^{16}C)$	–	2.6	1.4	1.6	2.3	1.6	2.3	2.7	–

[a] The ^{16}C state at 6.11 MeV is observed in ^{14}C(t,p) reactions [24,26].

the widths of the ^{16}C resonances are even always smaller than for the partner resonances in ^{17}C by about a factor of two.

A systematic behaviour is also observed in the ratio of cross sections $d\sigma(^{16}C)/d\sigma(^{17}C)$ for the pairs no. 2 - 6 (table 3, line 8). The first four pairs have an almost constant ratio of roughly 2.7 and the next pair of 1.5. Then, at higher excitation energies, the ratio decreases for the next pair to 0.6, but rises again to 1.6 at the end. The nearly constant ratio up to the pair no. 6 is shortly discussed in the following in a qualitative way. Again this observation may be understood on the basis of the same structure of the members of a pair with one strong $[(sd)^3]j^\pi$ configuration. The angular momentum dependent factors in the three-neutron transfer reaction are then the same for the members (except for the coupling to the core) and they drop out in the ratio of the cross sections.

The dynamical matching conditions affect the cross section also in a comparable way. Besides the effect of the angular momentum matching [31] the dependence on the linear momentum transfer and total Q-value of the compared reactions has to be considered. The ground state Q-values are different, -46.93 MeV, -39.48 MeV and -38.79 MeV for ^{17}C, ^{16}C and ^{15}C, respectively. However, when Q-values for the *corresponding* states are compared, they are almost equal. For example, for the three states in ^{17}C, ^{16}C and ^{15}C at 2.06 MeV, 7.74 MeV, 8.45 MeV (no. 2, table 3), the Q-values are -48.99 MeV, -47.22 MeV, -47.25 MeV, respectively. This means, that their total binding energy is approximately equal. Then also the grazing angular momenta in the exit channels, which are relevant for the dynamical matching conditions, are approximately equal for the three members and vary in a systematic way in dependence on the excitation energy.

The correspondence of states is further extended to ^{15}C as indicated in fig. 5 by the (red) lines. Here the states between 8.45 MeV and 19.0 MeV excitation energy are considered. At the beginning of the sequence the partner to the 6.11 MeV state of ^{16}C is not clearly identified in ^{15}C. It might be the weak state at 6.35 MeV, which was assigned $(5/2^+ - 9/2^+)$ [34], it is therefore listed in brackets in table 3, line 9. Beyond the highest-lying member of this group at 19.0 MeV, no further state is observed in the ^{15}C spectrum up to 26 MeV. The excitation energies are compared in detail in the lower part of table 3 to those of ^{17}C by subtracting the constant value of 6.65 MeV. Here the differences show a systematic trend from -0.30 MeV at the lowest-lying identified state at 8.45 MeV to +0.64 MeV at the highest-lying state of 19.0 MeV (table 3, line 11). The connecting lines between the spectra of ^{15}C and ^{16}C are not parallel anymore as this was the case for ^{16}C and ^{17}C.

The strongest peak in the ^{15}C-spectrum above the well known state at 6.84 MeV, which has a neutron 2p-1h structure, is found at 9.75 MeV. It clearly corresponds to the strongest peak in the ^{16}C spectrum (above 5 MeV) at 8.92 MeV and in the ^{17}C spectrum to the state at 3.10 MeV, which both have a stretched $[(1d5/2)^3]$ $9/2^+$ configuration. In ^{16}C the additional spin of the ν1p1/2 hole of the ^{13}C core couples to the final value $J^\pi = 5^-$ in the stretched configuration. For the ^{15}C state at 9.75 MeV we conclude from the correspondence in excitation energy and strength to the strongest states of ^{16}C and ^{17}C, that also this state has a stretched $[(1d5/2)^3]$ $9/2^+$ configuration, and it is assigned tentatively as $J^\pi = (9/2^+)$.

Table 4. Comparison of the structure of states of ^{15}C, ^{16}C and ^{17}C observed in the three-neutron stripping reaction (^{12}C,^{9}C) on ^{12}C, ^{13}C, and ^{14}C, respectively, at 231 MeV and comparison of experimental with SM-results for ^{17}C and ^{19}O calculated with the code Oxbash [47]. The following entries are shown in the table from left to right: tentative spin-parities J^π and experimental excitation energies E_x of ^{15}C states observed in this work, spin-parities (most are assigned tentatively) and experimental excitation energies of ^{16}C states, experimental excitation energies and spin-parities for ^{17}C states (tentative assignments, see text), SM-calculations for ^{17}C, known levels of ^{19}O, which correspond by their excitation energies and SM-structure to ^{17}C states, and theoretical excitation energies of ^{19}O from Oxbash-calculation. For the SM-calculations of ^{17}C five columns are given: J^π, excitation energies E_x, and the distribution of neutrons over the three j-levels 1d5/2, 2s1/2, 1d3/2 for each state (see also fig. 6). Bold printed excitation energies correspond to strong states. Excitation energies E_x are given in units of MeV.

	^{15}C		^{16}C		^{17}C		^{17}C					^{19}O		
	exp.[a]		exp. [27]		exp.[a]		calc.[a]					exp. [48]		calc.[a,f]
No.	J^π	E_x[b]	J^π	E_x	E_x	J^π	J^π	E_x	$1d\frac{5}{2}$	$2s\frac{1}{2}$	$1d\frac{3}{2}$	J^π	E_x	E_x
					0.00	$\frac{3}{2}^+$,[c]	$\frac{3}{2}^+$	0.00	**2.3**	0.5	0.2	$\frac{3}{2}^+$	0.096	0.29
					0.21[d]	$(\frac{1}{2}^+)$	$\frac{1}{2}^+$	0.31	1.8	1.0	0.2	$\frac{1}{2}^+$	1.47	1.57
1	$(\frac{5}{2}\text{-}\frac{9}{2})^+$	6.35	(3^-)	6.11[e]	0.31[a,d]	$\frac{5}{2}^+$	$\frac{5}{2}^+$	0.02	**2.3**	0.5	0.2	$\frac{5}{2}^+$	0.00	0.00
							$\frac{5}{2}^+$	2.06	1.6	1.3	0.1	$\frac{5}{2}^+$	4.71	5.29
							$\frac{1}{2}^+$	2.59	1.9	0.9	0.2	$\frac{1}{2}^+$	2.78	3.07
2	$(\frac{3}{2}^+\text{-}\frac{7}{2}^+)$	8.45	$(1^-\text{-}4^-)$	7.74	2.06	$(\frac{3}{2}^+,\frac{7}{2}^+)$	$\frac{3}{2}^+$	2.79	**2.1**	0.4	0.5	$\frac{3}{2}^+$	3.07	3.42
3	$(\frac{9}{2}^+)$	**9.75**	5^-	**8.92**	**3.10**	$\frac{9}{2}^+$	$\frac{9}{2}^+$	**3.00**	**2.4**	0.3	0.3	$\frac{9}{2}^+$	2.37	2.59
			(4^-)	9.42										
4	$(\frac{5}{2}^+\text{-}\frac{9}{2}^+)$	**11.05**	$(3^-,5^-)$	**9.98**	**4.25**	$(\frac{5}{2}^+\text{-}\frac{9}{2}^+)$	$\frac{5}{2}^+$	**4.11**	1.7	1.0	0.3	$\frac{5}{2}^+$	3.15	3.17
							$\frac{9}{2}^+$	**4.78**	**2.1**	0.7	0.2	$\frac{9}{2}^-\text{-}\frac{13}{2}^-$	5.38	5.32
							$\frac{7}{2}^+$	4.97	1.9	0.3	0.8	$(\frac{7}{2}^+)$		6.54
			$(2^-,4^-)$	10.39										
							$\frac{3}{2}^+$	4.32	1.5	0.9	0.6	$\frac{3}{2}^+$	4.11	5.04
							$\frac{1}{2}^+$	4.78	1.2	0.7	1.1	$(\frac{1}{2}^+)$		6.41
		11.8		11.08										
5	$(\frac{5}{2}^+)$	**13.1**	(3^-)	**11.85**	**6.20**	$(\frac{5}{2}^+)$	$\frac{5}{2}^+$	**6.68**	**2.0**	0.2	0.8	$(\frac{5}{2}^+)$		7.10
							$\frac{3}{2}^+$	6.12	1.4	0.6	1.0	$\frac{3}{2}^+$	5.54	
	$(\frac{5}{2}^+,\frac{7}{2}^+)$	13.8	$(2^-\text{-}4^-)$	12.54			$\frac{5}{2}^+$	6.30	1.4	0.5	1.1			
							$\frac{1}{2}^+$	7.44	1.6	0.6	0.8			
							$\frac{3}{2}^+$	7.14	1.1	1.1	0.8			
6	$(\frac{11}{2}^+)$	**14.57**	$(6^-,5^-)$	**13.12**	**7.47**	$(\frac{11}{2}^+)$	$\frac{11}{2}^+$	**6.84**	**2.0**	0.1	0.9	$\frac{7}{2}\text{-}\frac{11}{2}$	6.47	7.11
7		16.0		14.90	**8.85**		$\frac{9}{2}^+$	8.61	1.7	0.4	0.9			
							$\frac{9}{2}^+$	9.27	1.6	0.7	0.7			
							$\frac{7}{2}^+$	9.39	1.7	0.4	0.9			
8		17.8		**16.44**	**10.56**		$\frac{13}{2}^+$	10.17	2.8[g]	0.0	0.2			
9		19.0		17.4	11.71									
					12.61									
					13.70									
					(16.3)									

[a] this work [b] up to 11.8 MeV also from [34] [c] [16,19] [d] [14,15,20,21] and table 2 [e] [24,26] [f] see also [49] [g] $\nu(1d\frac{5}{2})^3 \otimes \pi 2^+$

To summarize this section we conclude from the extremely regular behaviour of the level distances for ^{17}C and ^{16}C over the energy range of more than 11 MeV, even with a comparable population profile, that the corresponding states must have very similar three-neutron configurations coupled to the ^{14}C and ^{13}C cores, respectively. This conclusion can be extended also to the discussed states of ^{15}C: the tentative spin-parity assignments can be continued for the corresponding observed states from ^{17}C and ^{16}C to ^{15}C, once the assignments have been made for ^{17}C. We will use this argument later for the interpretation of the measured partial angular distributions of ^{15}C states, where explicit configurations have to be used in the coupled channel calculations.

4.2 Shell model calculations for ^{17}C and comparison to ^{19}O

Shell model (SM) calculations had been performed already for the three lowest-lying states of ^{17}C by Warburton and Millener [16], which restricted the spin assignment for the ground state "model independent" to the values $1/2^+$, $3/2^+$. Later Ogawa *et al.* [19] used SM-calculations to compare the experimental g-factor of ^{17}C from their measurement to calculated g-factors of different configurations. In this way they could restrict the assignment for the ground state to $3/2^+$ by excluding $1/2^+$.

We performed in this study shell model calculations for ^{17}C up to about 10 MeV excitation energy. The observations discussed in the preceeding section strongly indicate, that according to the actual reaction conditions essentially (sd)^3 structures are populated on a core of ^{14}C. This core has a closed (1p) neutron shell with only small contributions from ground state correlations.

The latter aspect is very advantageous for theoretical investigations of the [(sd)$^3\otimes$ core] structures populated by the (^{12}C,^{9}C) reaction in ^{17}C. The same [(sd)$^3\otimes$ core] structures are also populated in ^{16}C and ^{15}C, where such a clear situation is not expected due to the hole-configurations in the neutron (1p) shell. In this approach we have also performed SM-calculations for ^{19}O, and we will compare the ^{17}C levels to the known levels of ^{19}O, which should have about the same (sd)^3 structures on a core of ^{16}O with a closed (1p) shell for neutrons and protons.

The SM-calculations have been restricted by the following conditions:
(1) for neutrons only $(sd)^3_{j^\pi}$ configurations are included,
(2) core excitations from the (1p) to the (sd) shell are for neutrons very weak and have been neglected (the neutron (1p) shell is closed),
(3) core excitations for protons are allowed within the (1p) shell: $\pi 2^+$ states coupled from the one- or two-proton excitations to the 1p1/2 shell (the lowest state is located at 7.01 MeV in ^{14}C), and $\pi 0^+$ states from two-proton excitations. Proton excitations from the (1p) to the (sd) shell have not been included.

Odd parity states are not obtained for ^{17}C within these conditions. Excitations to the (fp) shell are not considered here, because this would require calculations with a very large configuration space including the three major shells (1p), (2s1d), (1f2p). Such extended SM-calculations are beyond the scope of the present paper.

The SM-calculations have been performed using the code OXBASH [47] with the '*psdpn*' model space and single-particle energies and with the '*psdmwkpn*' interaction [12]. In the calculations for ^{17}C we checked in a few test cases the effect of (2p-2h) excitations from the *neutron* 1p1/2-shell to the (sd)-shell. We found that such contributions were very small, and in the further work the neutron (1p) shell was assumed to be closed.

The results of the SM-calculations for ^{17}C are given in table 4 together with the experimental results, and the corresponding level diagram is shown in fig. 6. The complete set of levels calculated according to the conditions (1) - (3) is given up to 9.5 MeV excitation energy in table 4. In addition the lowest lying $13/2^+$ state at 10.17 MeV has been included, which requires a 2^+ excitation of the proton configuration.

Table 5. States of ^{17}C with an *excited proton configuration* within the (1p) shell obtained in the SM-calculations up to 10.2 MeV excitation energy. The final spin J^π is coupled from $\pi 2^+ \otimes \nu j^\pi$. These states (except $13/2^+$) are not listed in table 4 and are also not shown in fig. 6. Proton occupancies are given in the (1p) shell and neutron occupancies in the (sd)-shell.

J^π	E_x	$\pi[(1p)^2]2^+$		$\nu[(sd)^3]j^\pi$		
	[MeV]	$3/2^-$	$1/2^-$	$\nu 5/2^+$	$\nu 1/2^+$	$\nu 3/2^+$
$1/2^+$	7.44	3.01	0.95	2.3	0.4	0.3
	9.92	3.00	1.00	2.4	0.4	0.2
$3/2^+$	8.16	3.11	0.86	2.2	0.5	0.3
	9.34	3.08	0.88	1.9	0.8	0.3
$5/2^+$	8.50	3.08	0.88	1.7	1.0	0.3
	8.85	3.22	0.74	1.7	0.7	0.6
	9.05	3.00	0.97	2.2	0.5	0.3
$7/2^+$	6.10	3.05	0.91	2.0	0.6	0.4
	9.01	3.12	0.85	2.0	0.6	0.4
	9.68	2.91	1.06	2.0	0.8	0.2
$9/2^+$	7.56	3.02	0.95	2.3	0.5	0.2
	9.68	3.02	0.95	1.9	0.9	0.2
$11/2^+$	9.50	2.93	1.04	2.1	0.7	0.2
$13/2^+$	10.17	2.94	1.03	2.8	0.0	0.2

In table 4 the list of excitation energies obtained from the SM-calculations follow the order of experimental excitation energies of ^{17}C (as far as available, including our results), taking already tentative spin assignments into account. Experimental excitation energies for levels of ^{19}O with known spins and even parity [48] are given in the second last column of table 4 and in the last column the result from the SM-calculations. These are ordered according to the same configurations as obtained for ^{17}C. In fig. 6 the states of ^{19}O are connected by lines with those of ^{17}C, when the calculated occupancies in the three neutron subshells agree within ± 0.2 units (with two exceptions: the lowest-lying $5/2^+$ and $9/2^+$ states, see below).

The neutron configurations in ^{17}C with (sd)^3 (3p-0h) structure couple to spins in the range from 1/2 to 11/2 and positive parity. In the weak coupling picture these configurations should be found in ^{19}O at low excitation energies, since ^{19}O has three neutrons outside the closed-shell ^{16}O core. Warburton [49] identified in SM-calculations, within the excitation energy range up to about 5.3 MeV for the experimentally known states of ^{19}O, those states, which have an (sd)^3 (3p-0h) structure (10 states). These are all reproduced in our calculations for ^{19}O, in agreement also with the experimental spin assignments given in [48] (see table 4, the 10 states for ^{19}O below 5.4 MeV).

The occupancies of the SM-orbits 1d5/2, 2s1/2, 1d3/2 are given in table 4 explicitely for each state. Except for the lowest-lying $5/2^+$ and $9/2^+$states, where the occupancy of the 1d5/2 shell is larger in ^{19}O by 0.4 units compared to ^{17}C, and for the $3/2^+$ states at 4.32 MeV in ^{17}C and 5.04 MeV in ^{19}O, all the entries in table 4 up

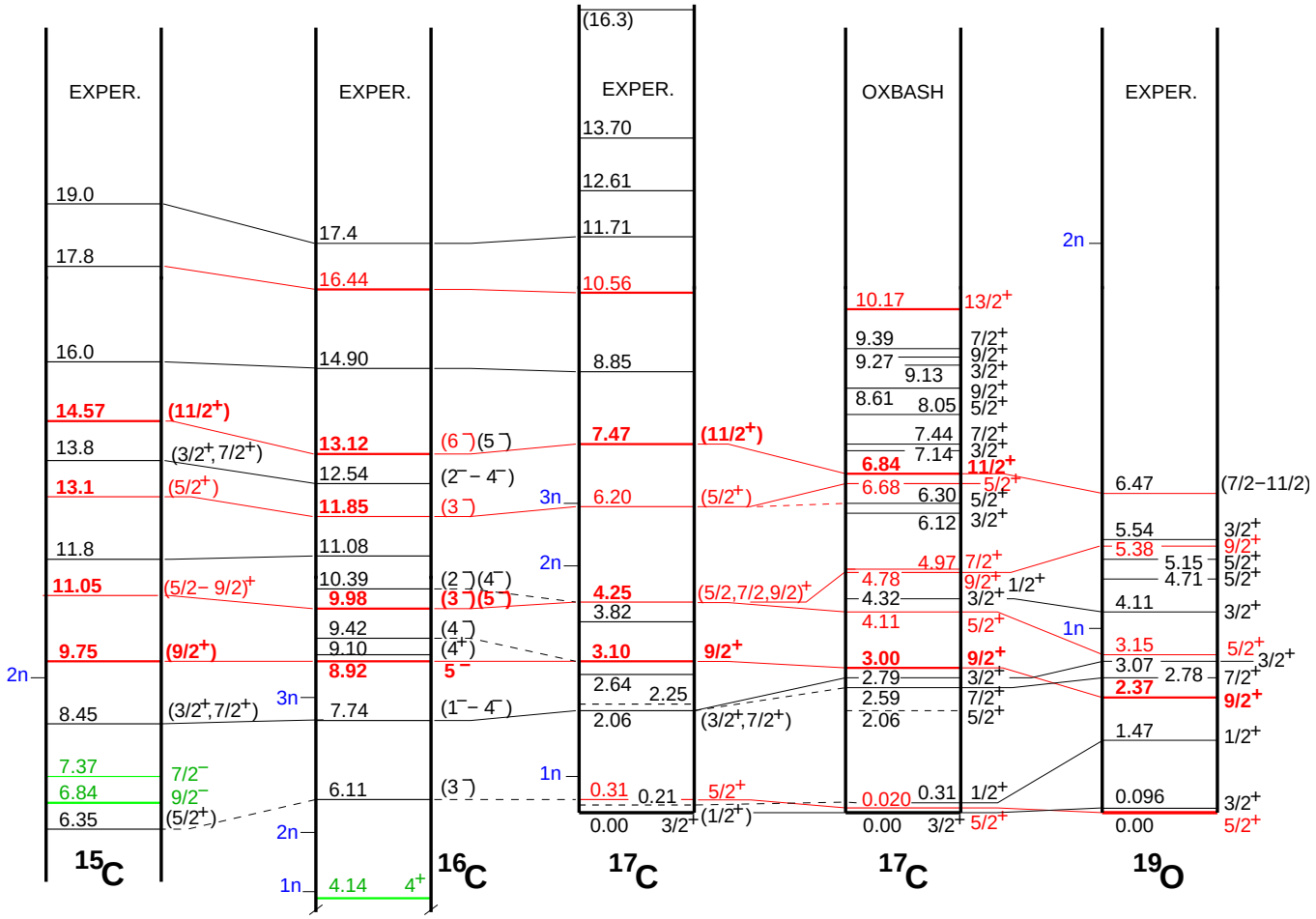

Fig. 6. (Color online) Comparison of experimental level schemes of ^{17}C (this work and [14,15,20–22]), ^{19}O [48], ^{16}C ([27] and refs. therein), ^{15}C (this work and [34]), and SM-calculations for ^{17}C using the code Oxbash [47] for neutron $(sd)^3$ configurations (see also tables 4, 5, 6). The experimental level scheme of ^{16}C is shifted by 5.82 MeV to align the 5^- state at 8.92 MeV to the $9/2^+$ state of ^{17}C at 3.10 MeV, and the level scheme of ^{15}C is shifted up by 6.65 MeV for the corresponding alignment of the 9.75 MeV state to the same state of ^{17}C. In the level scheme of ^{19}O only states with even parity are shown, and the state at 6.47 MeV. Neutron thresholds are indicated on the left of the experimental level schemes.

to 9 MeV shown for ^{17}C also have about the same values of occupancies for ^{19}O, with differences only up to 0.2 neutrons in any of the three shells. Therefore these occupancies are not repeated for ^{19}O in table 4. At even higher excitation energies the agreement of occupancies is not as perfect, but the parentage of configurations in both nuclei can still be recognized.

In the three-neutron transfer reaction the cross sections for populating $\nu(sd)^3$ configurations in combination with *one-proton* core excitations to $\pi 2^+$ configurations are expected to be strongly reduced due to the higher-order process. Therefore the states with such configurations are listed separately in table 5. One can see, that these states appear only above 7.3 MeV (one exception: a $7/2^+$ state at 6.10 MeV). In general, the inclusion of configuration mixing in the proton (1p) shell to the amount of typically 30-50% was important for all states to improve the agreement between experimental and calculated level energies (see condition (3)).

We want to discuss now details of the results from the shell model calculations. The calculated sequence of the $3/2^+_1$ state as the ground state of ^{17}C and then the $5/2^+_1$ state reproduces the experimental order of these states (fig. 6). The reversed order in ^{19}O obtained in [49] is also in agreement with the experimental data [48].

The $1/2^+_1$ state in ^{19}O calculated at an excitation energy of 1.57 MeV (experimental value: 1.47 MeV [48]) is shifted down by about 1.2 MeV in ^{17}C and appears at 0.31 MeV in the calculation, but experimentally it has not yet been clearly identified. The data obtained recently in the in-beam γ-spectroscopy of ^{17}C [20,21] show besides a strong line at 0.330(5) MeV, which corresponds to the excitation energy of the $5/2^+_1$ state, a weak γ-line at 0.210(5) MeV, which results most probably from the γ-decay of the $1/2^+_1$ state to the ground state.

The excitation energy of the $5/2^+_1$ state found in the latter measurements is located at slightly higher energy (0.330(5) MeV) as compared to the value observed by

Nolen *et al.* at 0.292(20) MeV [14], and Fifield *et al.* [15] at 0.295(10) MeV. We observe this state at 0.31(4) MeV and will continue to use this value for the $5/2^+_1$ state. From our measurement a tentative $(1/2^+)$ assignment for this state can be excluded by the argument, that the reaction mechanism would suppress a state with such a low spin and strong 2s1/2 component (table 4).

The next higher-lying state obtained in the SM calculations, which is located at an excitation energy of 2.06 MeV, has the strongest occupancy of the 2s1/2 shell (67%) of all states of the present calculations. An extremely small cross section can be expected for this configuration, and we assume, that this state is not observed in the (^{12}C,^{9}C) reaction on ^{14}C. The state no. 2 in table 4 *observed* at 2.06 MeV should therefore not be identified with this SM-state.

The calculated states of ^{17}C between 2.5 MeV and 5.0 MeV have relatively strong two-neutron $(1d5/2)^2$ terms, except the $3/2^+$ state at 4.32 MeV and the $1/2^+$ state at 4.78 MeV. At higher excitation energies up to about 10 MeV this strong 1d5/2 occupancy decreases on the average. In the region above 4.7 MeV the 1d3/2 shell has an increased occupancy of about one neutron in this shell for most of the states. The 1d3/2 single-particle strength is well known from ^{15}C as a broad $3/2^+$ resonance at 4.78 MeV [38]. In ^{17}C the main strength is obviously located at slightly higher excitation energies.

The occupancies of the 2s1/2 shell are distributed over the full range of calculated excitation energies, with fluctuations between 0.1 and 1.1 units. The maximum is reached for the pair of $5/2^+$ states in ^{17}C and ^{19}O at 2.06 MeV and 5.29 MeV, respectively, with 1.3 neutrons in the 2s1/2 shell, which is equivalent to a very strong $[(2s1/2)^2_{0^+} \otimes (1d5/2)]_{5/2^+}$ component in the wave function. The state in ^{19}O may be identified with one of the close-lying *observed* $5/2^+$ states at 4.71 MeV and 5.15 MeV [48]. These $5/2^+$ states have in ^{17}C and ^{19}O identical occupancies in all three shells, but the excitation energy calculated for ^{17}C is much lower. It seems to be a general feature, that the excitation energies of states with strong 2s1/2 configurations are shifted down in energy going from ^{19}O to ^{17}C. This is true for example for the pair of the first $1/2^+$ states in ^{19}O and ^{17}C and for most of the pairs of states, which show this behaviour in the calculated diagrams in fig. 6.

It is interesting to understand from the SM-calculations more details about the structure of low-lying states of ^{17}C, *i.e., about configuration mixing.* In table 6 the detailed structure of the lowest-lying state for each spin-parity from $1/2^+$ to $11/2^+$ is given. The occupancies of the neutron 1d5/2, 2s1/2, 1d3/2 shells are shown explicitely for the main three-neutron coupling terms in combination with the proton configurations. The latter are denoted by $\pi4$, $\pi3$, $\pi2$ characterizing the number of 1p3/2 protons in the wave function. For all states in table 6 the $\pi4$ configuration is by far the strongest with about 70% contribution, whereas the 2^+ excitation ($\pi3$) varies only from 9.4% to 14.2% and the contribution from the two-proton excitations to the 1p1/2 shell ($\pi2$) is always smaller than

Table 6. Shell model configurations for the *lowest lying* states of ^{17}C with spins and even parity J^π obtained in SM-calculations using the code Oxbash [47]. The three-neutron configurations are specified in column 5 by the percentage of the different terms contributing to the configurations of the state with occupation numbers in the three shells 1d5/2 (column 6), 2s1/2 (column 7) and 1d3/2 (column 8). In column 3 the proton part of these terms are denoted by $\pi4$, $\pi3$, $\pi2$ for the configurations $\pi(1p3/2)^4_{0^+}$, $\pi[(1p3/2)^3(1p1/2)^1]_{2^+}$ and $\pi[(1p3/2)^2(1p1/2)^2]_{0^+}$, respectively, and their percentage is given in column 4 as the sum of the corresponding neutron configurations in column 5.

J^π	E_x^{calc} [MeV]	protons	[%]	neutrons, occupancy [%]	1d5/2	2s1/2	1d3/2
$\frac{1}{2}^+_1$	0.312	$\pi4$	72.1	*65.0*	2	1	
				5.4		1	2
				1.7	1	1	1
		$\pi3$	12.3	9.9	2	1	
				2.4	3		
		$\pi2$	10.3	10.3	2	1	
$\frac{3}{2}^+_1$	0.000	$\pi4$	70.4	*32.2*	3		
				30.7	2	1	
				2.0	2		1
				5.5	1	1	1
		$\pi3$	9.6	5.6	3		
				4.0	2	1	
		$\pi2$	10.4	5.8	3		
				4.6	2	1	
$\frac{5}{2}^+_1$	0.020	$\pi4$	74.2	*47.2*	3		
				18.8	1	2	
				5.0	1		2
				3.2	2		1
		$\pi3$	9.4	5.3	3		
				1.9	2	1	
				2.2	2		1
		$\pi2$	10.1	8.0	3		
				2.1	1	2	
$\frac{7}{2}^+_1$	2.588	$\pi4$	76.9	*65.2*	2	1	
				7.4	1	1	1
				3.1	2		1
				1.2	1		2
		$\pi3$	10.1	2.8	3		
				1.5	1	2	
		$\pi2$	8.2	8.2	2	1	
$\frac{9}{2}^+_1$	2.995	$\pi4$	72.6	*39.0*	3		
				15.7	2	1	
				10.0	1	1	1
				7.9	2		1
		$\pi3$	13.0	6.1	3		
				2.3	2	1	
				2.1	1	1	1
				2.5	2		1
		$\pi2$	11.4	6.2	3		
				2.2	2	1	
				1.5	1	1	1
				1.5	2		1
$\frac{11}{2}^+_1$	6.840	$\pi4$	67.6	*67.6*	2		1
		$\pi3$	14.2	9.1	2		1
				2.7	2	1	
				2.4	1	1	1
		$\pi2$	9.4	9.4	2		1

11.5%. But with increasing excitation energies also the percentage of core excitations increases.

A single dominant configuration of neutrons is obtained in the cases of the lowest-lying states of spins $1/2^+$, $7/2^+$ and $11/2^+$ (table 6). These three states have a relatively simple structure, where the main term has a strength of 65%: no proton core excitation (π4), two neutrons in the 1d5/2 shell coupled to 0^+, 4^+ and 4^+, respectively, and the third neutron in the 2s1/2 shell for the two former states and in the 1d3/2 shell in the latter case to couple to the final spins $1/2^+$, $7/2^+$ and $11/2^+$, respectively. The configurations are: $[(1d5/2)^2_{0^+}\otimes(2s1/2)]_{1/2^+}$, $[(1d5/2)^2_{4^+}\otimes(2s1/2)]_{7/2^+}$, $[(1d5/2)^2_{4^+}\otimes(1d3/2)]_{11/2^+}$.

As pointed out already, the spin 11/2 can be reached with three neutrons in the (sd)-shell only by this coupling, other configurations without proton core excitations do not exist in that case. For the second $11/2^+$ state it turns out, that the core excited $[\pi 2^+ \otimes \nu 9/2^+]_{11/2^+}$ configuration has a strength of almost 90%. Such a strong core excitation shifts the excitation energy higher up to 9.50 MeV (table 5).

For the lowest $5/2^+$ and $9/2^+$ states a clear dominance of the $(1d5/2)^3$ configuration is found (table 6), in the former case with a $[(1d5/2)^2_{0^+}\otimes (1d5/2)]_{5/2^+}$ configuration (47%) and in the latter case with the stretched $(1d5/2)^3_{9/2^+}$ configuration (39%). The next largest terms include the 2s1/2 shell: the $[(2s1/2)^2_{0^+}\otimes(1d5/2)]_{5/2^+}$ configuration with 18.8% for the $5/2^+$ state, and for the $9/2^+$ state with two terms, 15.7% for $[(1d5/2)^2_{4^+}\otimes (2s1/2)]_{9/2^+}$ and 10% for $[(1d5/2\otimes 1d3/2)_{4^+}\otimes (2s1/2)]_{9/2^+}$. At higher excitation energies terms with the 1d3/2 shell become stronger.

Most interesting is the detailed structure of the ^{17}C ground state as a result of the SM-calculation. As one can see from table 6, the $3/2^+_1$ state receives only very small contributions from the 1d3/2 shell, about 7.5%. The main components are coupled from the 1d5/2 and 2s1/2 shells with about equal strengths: 32% for the $(1d5/2)^3_{3/2^+}$ component, and 31% for the equivalent couplings $[(1d5/2)^2_{2^+}$ $\otimes$ $(2s1/2)$ $]_{3/2^+}$ and $[(1d5/2\otimes 2s1/2)_{2^+}$ $\otimes$ $(1d5/2)$ $]_{3/2^+}$. This result has been obtained already in [6]. In these terms two of the three neutrons have to be coupled to 2^+, which implies a strong quadrupole deformation (in the $(1d5/2)^3_{3/2^+}$ term also the coupling of two neutrons to 4^+ is possible). In ^{16}C the corresponding 2^+ states with these configurations are identified at 1.77 MeV and 3.98 MeV, and the 4^+ state at 4.14 MeV [25]. The next terms with proton core excitations (table 6) add about 10% more strength to both neutron configurations. These SM-results for the ^{17}C ground state are in very good agreement with the experimental results obtained from one-neutron-removal reactions measured in coincidence with γ-transitions in ^{16}C by Maddalena *et al.* [6] and Datta Pramanik *et al.* [7].

Finally we want to discuss shortly ν(4p-1h) structures of odd parity in ^{17}C and corresponding ν(2p-1h) structures in ^{15}C. The former could be populated in the ^{14}C(^{12}C, ^{9}C)^{17}C reaction only by a second-order process via the ν(1p-1h) core excitations of ^{14}C, whereas the latter are directly accessible in the 3n-transfer on ^{12}C. However, the lowest-lying odd-parity states in ^{15}C with this structure, which are located at 3.103 MeV ($1/2^-$), 4.22 MeV ($5/2^-$) and 4.66 MeV ($3/2^-$), are extremely weakly populated (fig. 1, lower and upper panels). Then the structures in ^{17}C must be populated even with smaller strength due to the required higher-order process of the core excitation.

We performed SM-calculations for states of ^{17}C with odd parity and obtained excitation energies and spins for the three *lowest-lying* states of 2.47 MeV, $1/2^-$; 3.77 MeV, $5/2^-$; and 4.52 MeV, $3/2^-$. These states have indeed a ν(4p-1h) structure with a hole in the 1p1/2 neutron shell, and they correspond most probably to the three states observed in the β-decay of ^{17}B [22] (see sect. 1 and table 2, lower part). Therefore we suggest the following tentative assignments for the observed states [22]:
(2.25 MeV), ($1/2^-$); 2.64 MeV, ($5/2^-$); 3.82 MeV, ($3/2^-$).

4.3 Discussion of assignments for ^{17}C (and ^{16}C)

In this section we want to summarize the tentative assignments for the resonances observed in the ^{17}C spectrum using arguments from:
(i) the sensitivity of cross sections on dynamical matching conditions for specific configurations in combination with results from SM-calculations;
(ii) the systematic agreement of excitation energies between the observed states of ^{17}C, ^{16}C and ^{15}C (except a constant shift) and of further properties of these states;
(iii) the information from the comparison of ^{19}O and ^{17}C taking experimental data and SM-calculations into account.

Since we observe a strong correlation between the states of ^{17}C and ^{16}C in several respects, we will include also the corresponding ^{16}C states in the discussion for the assignments. In principle, for every state of ^{17}C with a (sd)^3 (3p-0h) configuration there exists in ^{16}C a *doublet* of states with a (3p-1h) configuration, where the neutron 1p1/2-hole in the ^{13}C core couples with parallel and anti-parallel orientation to the spin of the (sd)^3 configuration. The parallel spin coupling to J_{max} is much more favoured by the dynamical matching conditions compared to the anti-parallel coupling. Therefore only the state and assignment with parallel coupling is discussed (see details also in [27]).

0.00 MeV, 3/2$^+$, (not observed in this reaction)

The structure of the ground state of ^{17}C has been discussed already in the previous subsection and in connection with table 6. Only a small cross section is expected due to the anti-parallel coupling between the ^{16}C(2^+) core and the 2s1/2 or 1d5/2 neutron. A peak could not be identified in the spectrum.

0.21 MeV, (1/2$^+$), (not observed in this reaction)

In the in-beam γ-spectroscopy of ^{17}C two γ-lines were found [20,21]: a weak line at 0.210(5) MeV and a strong line at 0.330(5) MeV. The latter is identified as the strong

state at 0.292(10) MeV in refs. [14,15] and at 0.31(4) MeV in our data. In the region of particle-stable states three states are expected from SM-calculations, their spins and parities are $1/2^+$, $3/2^+$, $5/2^+$. Since the latter two assignments are given to the ^{17}C ground state and the 0.31 MeV state, respectively, only this state at 0.21 MeV remains for the tentative $1/2^+$ assignment. In the (^{12}C,^{9}C) reaction a very small cross section is expected for a $1/2^+$ state and, in fact, it is not observed. A corresponding weak peak would be hidden in any case in the tail of the stronger peak of the $5/2^+$ state at 0.31 MeV.

0.31 MeV, $5/2^+$

This state is the third particle-stable state of ^{17}C (besides the ground state and the 0.21 MeV state), all other states at higher excitation energies are lying above the neutron threshold (S_n= 0.73 MeV) and are therefore unbound. The strength of the peak in our spectrum indicates a strong population of 1d5/2 orbits by the transferred neutrons. However, the 0.31 MeV state is not the strongest state in the spectrum (this would have been a signature for a stretched $(1d5/2)^3_{9/2^+}$ configuration in this reaction). Therefore we expect a coupling to a lower spin, $5/2^+$. Other reactions [14,15], where ^{17}C is detected as outgoing particle and therefore only bound states can be observed, also find a strong state at about the same excitation energy (table 2). The shell model predicts (besides the $3/2^+$ ground state and a $1/2^+$ state at 0.31 MeV) the lowest-lying $5/2^+$ state at 0.02 MeV, which has a dominant $(1d5/2)^3_{5/2^+}$ configuration. The corresponding $5/2^+$ state in ^{19}O is the ground state. These arguments support the $5/2^+$ assignment of this state.

The corresponding partner state in ^{16}C (table 3) is most probably the state at 6.11 MeV observed by Fortune *et al.* [24] and Sercely *et al.* [26] with tentative assignments of (2^+, 3^-, 4^+). From our results we would restrict this to (3^-), with an aligned coupling of the corresponding $5/2^+$ state of ^{17}C and the $1/2^-$ spin of the $^{13}C_{g.s.}$ core.

2.06 MeV, ($3/2^+$,$7/2^+$)

Using the results of the SM-calculations as a guide line at low excitation energies there are only two possible assignments for this state. These are the $7/2^+$ and $3/2^+$ SM-states at 2.59 MeV and 2.79 MeV, respectively. A further $5/2^+$ SM-state at 2.06 MeV is expected to be "invisible" in our reaction due to its very large $(2s1/2)^2$ component in the wave function. The corresponding state in ^{19}O *with the same calculated $(sd)^3$ structure* is located at much higher excitation energy (experiment: 4.71 MeV, calculation: 5.29 MeV), whereas the $7/2^+$ and $3/2^+$ states are located in ^{19}O at 2.78 MeV and 3.07 MeV, respectively. A tentative assignment of ($3/2^+$, $7/2^+$) is therefore given to this state.

In ^{16}C the corresponding partner state is found experimentally at 7.74 MeV (tables 3, 4, and ref. [27]). The coupling of the ($3/2^+$, $7/2^+$) configurations discussed for ^{17}C to the $1/2^-$ ground state of ^{13}C allows a range of possible spin assignments from 1^- to 4^-. In ref. [27] coupled-channel calculations have been performed for partial angular distributions assuming assignments of 1^-, 2^- and 3^-, and a preference for 3^- was deduced. We include also 4^- for a tentative assignment of this state, based on the parallel coupling of the $7/2^+$ configuration to the $1/2^-$ $^{13}C_{g.s.}$ core.

3.10 MeV, $9/2^+$

The $9/2^+$ assignment of this state is based on several arguments. First of all the peak has the largest cross section in the spectrum, which indicates clearly a stretched three-neutron $(1d5/2)^3$ configuration. We recall that for the same reason the 8.92 MeV state in ^{16}C had been assigned as 5^- [27]. Second, the SM-calculations predict the lowest $9/2^+$ state in ^{17}C at 3.00 MeV, almost at the experimental value. Third, in ^{19}O the theoretical and experimental values of the lowest $9/2^+$ state are found at 2.59 MeV and 2.37 MeV, respectively, which is also in very good agreement.

4.25 MeV, ($5/2^+$, $7/2^+$, $9/2^+$)

This narrow and well separated state is difficult to assign only from arguments deduced from the SM-calculations. Three SM-states with the spins and even parity $5/2^+$ (4.11 MeV), $7/2^+$ (4.97 MeV), $9/2^+$ (4.78 MeV) can be taken into account, with a preference for the higher spin states with strong (1d) shell occupancies. In ^{19}O states with corresponding structure are observed at 3.15 MeV for the $5/2^+$ and at 5.38 MeV for the $9/2^+$ states. The latter state is assigned (9/2 - 13/2) in the literature [48].

The corresponding state in ^{16}C at 9.98 MeV receives in this case the tentative assignments (3^-, 5^-), and the 10.39 MeV state, which is the anti-parallel coupling partner in ^{16}C, the values (2^-, 4^-).

6.20 MeV, ($5/2^+$)

There is a gap of almost 2 MeV between this state and the closest lower-lying state, which seems to be related to a change in the structure. In fact, the SM-calculations show now a much stronger occupancy of the 1d3/2 shell with about *one* neutron on the average (table 4). This is true for a number of states in this region up to the spin 11/2. According to the smaller observed cross section we suggest an assignment of ($5/2^+$). From the two $5/2^+$ states in the region around 6.20 MeV the state at 6.68 MeV is the best candidate, because it has occupancies of two neutrons are in the 1d5/2 shell and almost one neutron in the 1d3/2 shell, whereas the SM $5/2^+$ state at 6.68 MeV has much less strength in the 1d5/2 shell. The state in ^{19}O with approximately *the same SM-configuration* is found at 7.10 MeV (fig. 6).

The cross sections of the corresponding doublet in ^{16}C at 11.85 MeV and 12.54 MeV differ by a factor of three [27], which emphasizes again the importance of the correct choice for the configurations of these states. The 11.85 MeV state is therefore tentatively assigned as (3^-) with the parallel spin coupling ($5/2^+ \otimes 1/2^-$), and the 12.54 MeV state as (2^-), because it may be the coupling member of the latter configuration with anti-parallel spin orientation.

7.47 MeV, (11/2$^+$)

This strong resonance has the second largest cross section (table 2) observed in the ^{17}C spectrum (fig. 5), it must have a stretched configuration with high spin. It is also situated within the region of states, where the SM-calculations predict a strong contribution of the 1d3/2 shell. The $(1d5/2)^2_{4^+} \otimes (1d3/2)^1$ configuration allows for a maximum spin of $11/2^+$. In the SM-calculations the lowest-lying $11/2^+$ state is predicted at 6.84 MeV (table 4), not far from the experimental excitation energy. All these arguments favour a tentative assignment of this state as $(11/2^+)$. In ^{19}O the first $11/2^+$ state is found in the present SM-calculations at 7.11 MeV, and the (7/2 - 11/2) assignment of a state at 6.47 MeV observed in the ^{13}C(^{7}Li,p)^{19}O reaction [50] is in agreement with this. In ^{16}C the coupling of the $1/2^-$ core to the stretched $11/2^+$ configuration results in tentative assignments $(6^-, 5^-)$ for the corresponding state at 13.12 MeV.

8.85 MeV

For the assignment of this state only arguments deduced from cross sections and from the comparison of experimental excitation energies to the results of the SM-calculations can be used. We assume that at these higher excitation energies only states with higher spins can be observed in this reaction. The SM-calculations predict two $9/2^+$ states nearby at 8.61 MeV and 9.27 MeV, therefore this spin-parity is suggested as the most probable assignment. The corresponding state of ^{16}C is observed at 14.90 MeV (table 3).

10.56 MeV

No explicit assignment is given for this state in table 4. The best candidate from the SM-calculations is a $13/2^+$ high-spin state at a calculated excitation energy of 10.17 MeV (table 5), which is coupled from a stretched neutron $(sd)^3$, $9/2^+$, configuration and a proton 2^+ core-excitation. In a weak-coupling model an excitation energy of E_x= 3.10 + 7.01 MeV = 10.11 MeV would be expected using the lowest-lying states, $\nu 9/2^+$ of ^{17}C, and $\pi 2^+$ of ^{14}C, coupled to $13/2^+$. The relatively strong population of this state would be in agreement with the assignment of the high-spin value.

11.71 MeV and higher

Assignments for this state and higher-lying states are not given in table 4, because the identification of their structure is difficult due to the larger variety of possible contributing configurations at these high excitation energies. Nevertheless, we still find for this state the corresponding partner states in ^{16}C at 17.4 MeV and in ^{15}C at 19.0 MeV, which follow the same regular behaviour of excitation energies as discussed in connection with table 3. A common structure of $(sd)^3$ configurations is assumed for all these states.

For the ^{17}C states at 12.61 MeV, 13.70 MeV and 16.3 MeV no corresponding partner states of ^{16}C could be observed due to the limited excitation energy range, which was measured only up to 18 MeV. For ^{15}C the experimental spectrum extends up to 26 MeV, but no further state is found above 19 MeV.

4.4 ^{15}C assignments and angular distributions

For ^{15}C the assignment of states observed in the ^{12}C(^{12}C, ^{9}C) reaction was discussed so far only with a few remarks. However, from the consistent interpretation of the structure of states for ^{17}C and ^{16}C and from the observation, that approximately the same regular behaviour occurs for the ^{15}C states listed in table 3, it is concluded, that these states also have a particle-hole structure with three neutrons in the (sd)-shell, very similar to the corresponding states in ^{17}C and ^{16}C. In this case the core has two holes in the neutron (1p) shell corresponding to the 0^+ ground state of ^{12}C. The assignments proposed for ^{17}C should therefore also apply to the ^{15}C states with the corresponding structure (table 3), they are given in table 4.

Further support for the assignments of ^{15}C states can be deduced from the analysis of angular distributions obtained in the previous measurement of the ^{12}C(^{12}C,^{9}C)^{15}C reaction (lower panel of fig. 1). The partial angular distributions obtained for seven excited states of ^{15}C are shown in fig. 2 together with coupled channel calculations performed with the code Fresco [33] according to the coupling scheme of fig. 7. Here we used, except for the first two states at 6.84 MeV and 7.37 MeV, which have a (2p-1h) structure and odd parity [27], the $(sd)^3$ configurations with the main components and assignments as discussed for the corresponding states of ^{17}C. In this way the consistency of the tentative J^π assignments given in table 4 is checked.

The three-neutron transfer is treated in these calculations as a two-step process with a one-neutron transfer to ^{13}C states in the first step and a two-neutron transfer to final states of ^{15}C in the second step and vice versa, with the two-neutron transfer to states of ^{14}C in the first step and the one-neutron transfer in the second step. In this way always two transition amplitudes are obtained for each final configuration. The transition amplitudes of both transfer branches are added coherently for the calculation of the cross section.

The optical potential, which is defined as

$$U = V_0\ f_r(R) + i\ W_0\ f_i(R), \qquad (4)$$

is calculated using Woods-Saxon form factors

$$f_{r,i}(R) = [1 + exp\{(R - R_{r,i})/a_{r,i}\}]^{-1}. \qquad (5)$$

The potential parameters are taken from ref. [51] (parameter set WS2, ^{12}C-beam).

Only main configurations were included for the intermediate states: the single-particle states of ^{13}C (excitation energies in brackets): 1p1/2 (0.00 MeV), 2s1/2 (3.09 MeV), 1d5/2 (3.85 MeV), 1d3/2 (8.20 MeV), and the ^{14}C states: 0^+_2 (6.59 MeV), 2^+_2 (8.32 MeV), 4^+_1 (10.74 MeV), 3^-_1 (6.73 MeV). These are given in the lower part of table 7 as parts of the full configurations.

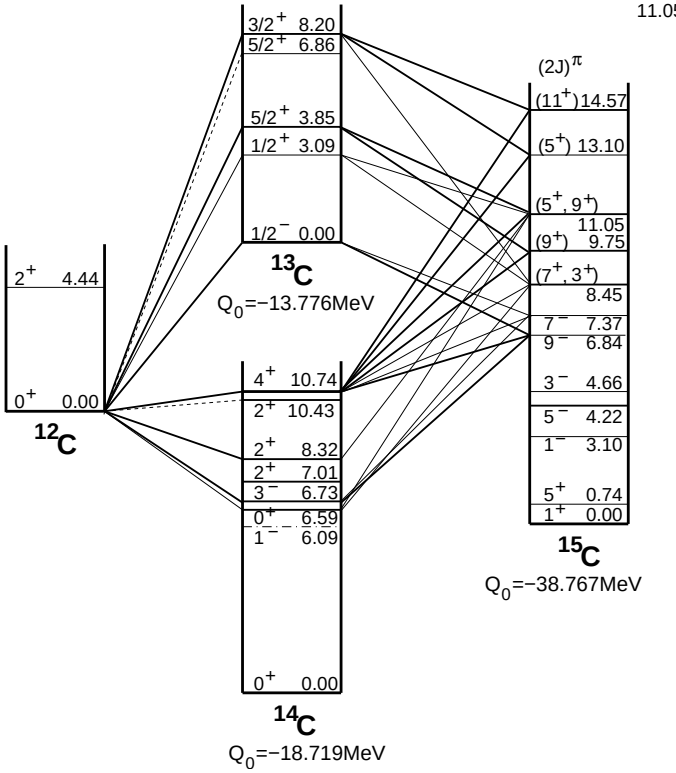

Fig. 7. Two-step coupling scheme for the target transitions in the ^{12}C(^{12}C,^{9}C)^{15}C reaction used in the coupled-channel calculations. The transitions through the corresponding intermediate states of ^{13}C and ^{14}C are shown.

Expected values of strength factors SF, which represent the product of the spectroscopic factors in the projectile and target systems, are of the order of one and can be estimated as follows (values were partly taken from Cohen and Kurath [52] and partly from previous work [27]).
Projectile transitions:
$C^2S\{^{12}C_{g.s.} = {}^{11}C_{g.s.} \otimes \phi_{1n}(1p3/2)\} = 5.7$
$C^2S\{^{11}C_{g.s.} = {}^{10}C_{g.s.} \otimes \phi_{1n}(1p3/2)\} = 0.7$
$C^2S\{^{10}C_{g.s.} = {}^{9}C_{g.s.} \otimes \phi_{1n}(1p3/2)\} \approx 1.0$
Target transitions via the ^{13}C, $5/2^+_1$, single-particle state:
$C^2S\{^{13}C_{5/2^+} = {}^{12}C_{g.s.} \otimes \phi_{1n}(1d5/2)\} = 0.7$
$C^2S\{^{15}C_{J^+} = {}^{13}C_{5/2^+} \otimes \phi_{2n,j}[(sd)^2_j$, j=0,2,4] $\} \approx 0.2-1.0$
For the other single-particle states of ^{13}C the spectroscopic factors are of similar strength as for the $5/2^+_1$ state [34].
Target transitions via ^{14}C states:
The same factors are used for the transition amplitudes of the 2n-stripping via ^{14}C states in the first step and the 1n-stripping in the second step, and the coherent sum of both transition amplitudes is calculated.
Values for a single transfer branch result in the range $SF_{s.t.b.} \approx 0.6-2.8$.

When the two transition amplitudes have about equal strength to a final state of ^{15}C via ^{13}C and via ^{14}C, a factor up to four can be gained for the final cross section in case of a constructive interference. In this case the strength factor SF, which is needed for the fit of the experimental cross section, is reduced by this factor (up to four) with respect to the estimate for a single transfer branch.

Table 7. Excited states of ^{15}C, for which partial angular distributions (fig. 2) have been analyzed in terms of coupled channel calculations. The following entries are given from left to right: excitation energies, spin-parities, couplings and strength factors SF (see text), excitation energies of corresponding states of ^{17}C and tentative assignments to these states from this work.

^{15}C				^{17}C	
E_x [MeV]	J^π	coupling $\phi_{1n}\otimes\phi_{2n}$	SF	E_x [MeV]	J^π
6.84	$\frac{9}{2}^-$	$1p1/2 \otimes 4^+_1$	0.1	–	
		$1d5/2 \otimes 3^-_1$	(9.0)	–	
7.37	$\frac{7}{2}^-$	$1p1/2 \otimes 4^+_1$	0.8	–	
8.45	$(\frac{3}{2}^+)$	$1d3/2 \otimes 0^+_2$	3.5	2.06	$(\frac{3}{2}^+)$
	$(\frac{5}{2}^+)$	$2s1/2 \otimes 4^+_1$	0.5		$(\frac{5}{2}^+)$
9.75	$(\frac{5}{2}^+)$	$1d5/2 \otimes 4^+_1$	1.7	3.10	$(\frac{5}{2}^+)$
11.05	$(\frac{5}{2}^+)$	$2s1/2 \otimes 4^+_1$	0.9	4.25	$(\frac{5}{2}^+)$
	$(\frac{5}{2}^+)$	$1d5/2 \otimes 0^+_2$	(9.0)		$(\frac{5}{2}^+)$
13.10	$(\frac{5}{2}^+)$	$1d3/2 \otimes 4^+_1$	(44)	6.20	$(\frac{5}{2}^+)$
14.57	$(\frac{11}{2}^+)$	$1d3/2 \otimes 4^+_1$	0.35	7.47	$(\frac{11}{2}^+)$

This is the case for example for the cross section of the $9/2^-$ state of ^{15}C at 6.84 MeV (upper part of table 7), which is described by the coupling $1p1/2 \otimes 4^+_1$ for the first and second transfer step in the first transition branch in this order (upper part of fig. 7), and vice versa for the second transition branch (lower part of fig. 7). In fact, the cross section is reduced by a factor between three and four, when the first or the second branch is switched off in the calculation. The interference effect therefore explains the relatively small strength factor of SF= 0.1.

We tested also a further possible contribution for the transitions to this state, in the first branch by a $1d5/2 \otimes 3^-_1$ coupling and in reverse order for the second branch. However, the resulting cross sections are a factor of *ninety* smaller compared to the ones for the $1p1/2 \otimes 4^+_1$ coupling and can be neglected in the calculation.

The $7/2^-$ coupling partner of the ($9/2^-$, $7/2^-$) doublet at 7.37 MeV with anti-parallel coupling of the $1/2^-$ neutron hole to the 4^+ two-neutron configuration has an about a factor of ten lower experimental cross section, which is also observed in the calculation (with an additional reduction factor of eight). This shows that the cross sections are rather sensitive to configurations and interference effects.

In the lower part of table 7 results are given for the five states of ^{15}C at 8.45 MeV, 9.75 MeV, 11.05 MeV, 13.1 MeV, 14.57 MeV, which are considered to have approximately the same three-neutron configurations as the corresponding states of ^{17}C at 2.06 MeV, 3.10 MeV, 4.25 MeV, 6.20 MeV, 7.47 MeV (table 3).

For the 8.45 MeV state two options for the assignment were deduced from the correspondence to ^{19}O states and from the SM calculations (table 4), namely $3/2^+$ with a dominant configuration $[(1d3/2) \otimes (1d5/2)^2_{0^+}\ ]_{3/2^+}$, and $7/2^+$ with a configuration $[(2s1/2) \otimes (1d5/2)^2_{4^+}\ ]_{7/2^+}$. In the coupled channel calculations only these main compo-

nents were taken into account using the couplings 2s1/2 $\otimes$ 4_1^+ and 1d3/2 $\otimes$ 0_2^+, respectively.

The corresponding calculated angular distributions of the 8.45 MeV state are shown in fig. 2 as dashed and solid lines, respectively. The data indicate a minimum in the angular distribution at about 11^o, which is reproduced by the angular distribution for the $3/2^+$ configuration. The normalization factor SF = 3.5 is also still acceptable. But the error bars of the data points are rather large and do not exclude completely a $(7/2^+)$ assignment, although this angular distribution has only a smoothly decaying shape. Therefore we keep both options, $(3/2^+)$ and $(7/2^+)$ for the assignment. Garrett *et al.* [35] suggested in the ^{9}Be(^{7}Li,p) reaction at 20 MeV incident energy for this state (at E_x=8.495 MeV in ref. [35]) a range of spin values from (9/2) to (13/2) from cross section systematics. From our analysis we would not assign a higher spin value than $7/2^+$.

A similar situation is met for the interpretation of the angular distribution of the ^{15}C state at 11.05 MeV, where the assignments $9/2^+$ and $5/2^+$ were suggested in the discussion above. The spin-parity $9/2^+$ is obtained from the stretched $[(2s1/2) \otimes (1d5/2)^2_{4^+}]_{9/2^+}$ configuration, whereas a $[(1d5/2) \otimes 0_2^+]_{5/2^+}$ coupling is assumed for the $5/2^+$ assignment. We deduce from the strength factors a preference for $9/2^+$, because the corresponding factor of SF=0.9 agrees well with the predictions, while the factor for the $5/2^+$ configuration is rather large (SF=9). An even much larger value (SF=44) is obtained for the strength factor of the next state at 13.10 MeV, which is assigned tentatively as $5/2^+$ with a $[(1d3/2) \otimes (1d5/2)^2_{4^+}]_{5/2^+}$ configuration (compare table 4). The large discrepancy may be related to the anti-parallel coupling of the discussed configuration. We have seen already for the $7/2^-$ state at 7.37 MeV a strong reduction of the calculated cross section due to this effect.

The angular distributions of the states with stretched configurations $[(1d5/2) \otimes (1d5/2)^2_{4^+}]_{9/2^+}$ at 9.75 MeV and $[(1d3/2) \otimes (1d5/2)^2_{4^+}]_{11/2^+}$ at 14.57 MeV are well reproduced by the calculations (fig. 2). Also the strength factors SF=1.7 and SF=0.35, respectively, are in good agreement with the expectations. The state at 9.75 MeV was assigned by Garrett *et al.* [35] as (9/2 - 13/2). From our analysis we obtain $(9/2^+)$ as the most probable assignment.

4.5 Decay properties and widths

The structures, which are populated in ^{17}C by the (^{12}C,^{9}C) reaction, have been characterized as neutron (3p-0h) configurations. In ^{16}C the (^{12}C,^{9}C) reaction populates the corresponding (3p-1h) configurations and in ^{15}C (3p-2h) configurations, respectively.

The (3p-0h) resonances of ^{17}C decay by one-neutron emission to (2p-0h) states of ^{16}C. These are well known from (t,p) reactions [24–26]. The same applies to the neutron decay of the (3p-1h) resonances in ^{16}C to (2p-1h) states of ^{15}C, which are also known from (t,p) reactions [36]. And it is clear, that the neutron-decay of (3p-2h) states of ^{15}C leads to states of ^{14}C with (2p-2h) character, which are discussed in refs. [25,32]. The regularities observed for the widths, as demonstrated in table 3, are related to the parentage of the structures between the parent and daughter states of the decay.

The corresponding neutron decays are shown in fig. 8. Here the level scheme of ^{16}C is shifted up to align the ground state of ^{16}C with the one-neutron threshold of ^{17}C at 0.73 MeV. In this way it is easy to see, how the excitation energies $E_{x,f}$ and spin-parities J^π_f of the ^{16}C states fit to possible decay branches, which are relevant for the regularities. In the decay from a given parent state ($E_{x,i}$, J^π_i) the neutron is emitted with the quantum numbers of its shell-model orbit j^π. Since this condition restricts the vector difference $|\mathbf{J}^\pi_i - \mathbf{J}^\pi_f| = |\mathbf{j}^\pi|$ to $1/2^+$, $3/2^+$, $5/2^+$ depending on its shell-model state 2s1/2, 1d3/2, or 1d5/2, respectively, only distinct daughter states ($E_{x,f}$, J^π_f) will fit. The transitions are specified in table 8, where the initial and final excitation energies and spin-parities, respectively, and the *decay energies at resonance (the resonance energies)*, E_R and E^*_R, are given. The former is defined by the decay to the ground state of the daughter nucleus and the latter by

$$E^*_R(J^\pi_i, J^\pi_f) = E_{x,i}(J^\pi_i) - S_n - E_{x,f}(J^\pi_f). \qquad (6)$$

The decay is restricted in addition by the conditions, that the spin-coupling factor $(\ell\ \mathbf{s} \mid \mathbf{j})(\mathbf{J_i}\ \mathbf{j} \mid \mathbf{J_f})$, which contains the decay angular momenta ℓ and $\mathbf{j}$, is non-zero and, that the parity is conserved. The decay energy as a free variable, E_{dec}= E_x - S_n, used formerly in the eqs. (1)-(3) for the Breit-Wigner resonances has to be replaced by

$$E^*_{dec}(J^\pi_i, J^\pi_f) = E_x - S_n - E_{x,f}(J^\pi_f) \qquad (7)$$

in this more general formulation. The daughter nucleus in the excited state $E_{x,f}(J^\pi_f)$ is considered as the core for the neutron decay, the decay energy is correspondingly reduced.

The resonance energies E_R or E^*_R for the neutron decay to the ground state or to an excited state of the daughter nucleus, respectively, can be compared in columns 4 and 8 of table 8. The differences are rather large in many cases. The effect on the line shape is shown in fig. 5, where the Breit-Wigner resonances are calculated using E^*_R, whereas E_R is used in figs. 1 and 3.

For low decay energies E^*_R , especially for the ^{16}C resonances no. 2 and 3, the tails of the resonances at the high excitation energy side are more extended due to the different energy dependences of the penetrabilities. However, the resonance positions agree within 10 keV with those obtained in the first analysis (figs. 1 and 3), and the widths are the same.

In some cases decay branches to two different final states are given in table 8 (see also fig. 8). These are the states at 6.20 MeV for ^{17}C, 9.98 MeV and 12.54 MeV for ^{16}C, and 13.1 MeV and 14.57 MeV for ^{15}C.

We discuss now a few details in the decay scheme of fig. 8. The $9/2^+$ state of ^{17}C at 3.10 MeV is expected to decay to the 2_1^+ state of ^{16}C by the emission of a neutron

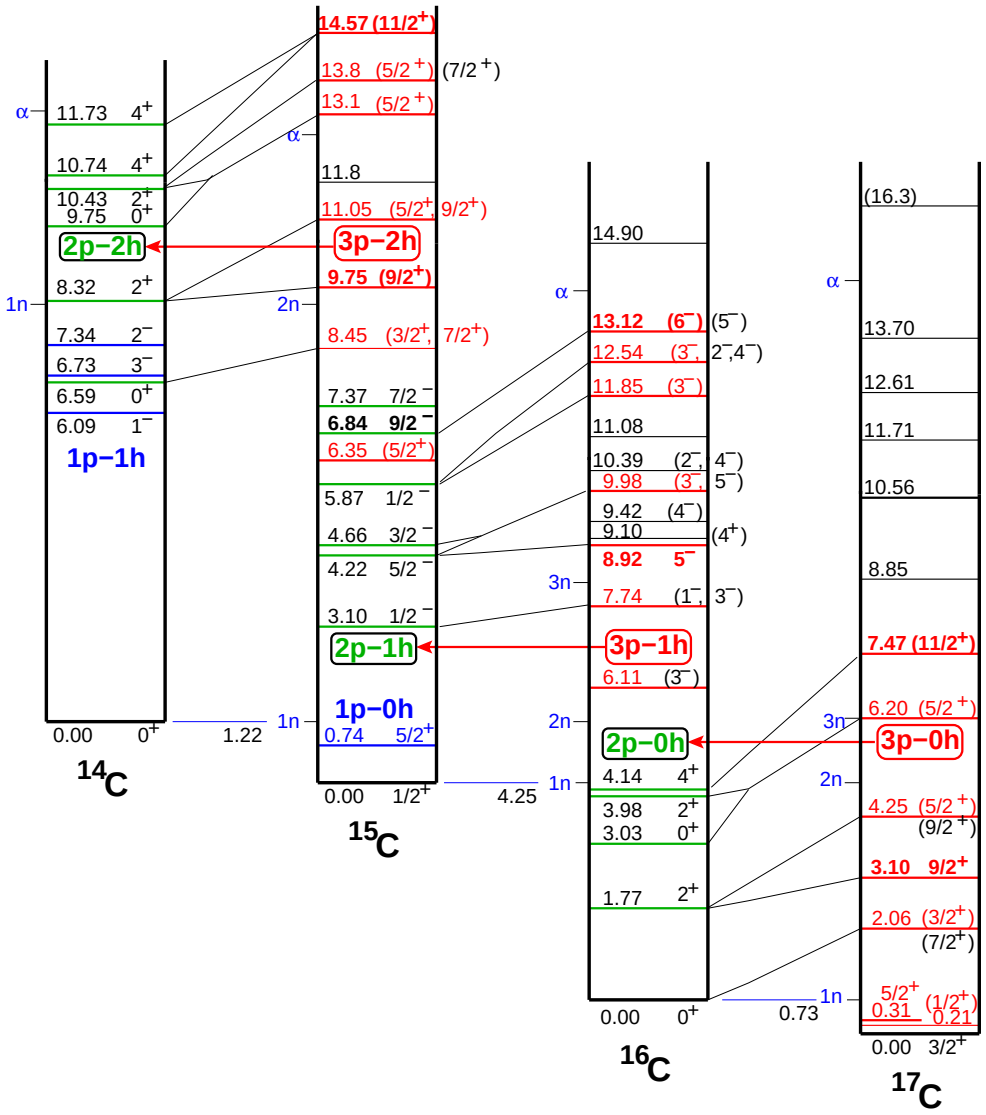

Fig. 8. (Color online) Decay schemes for the one-neutron decay of (sd)^3 structures in ^{15}C, ^{16}C and ^{17}C proposed from the systematics of excited states and from the interpretation of their widths given in table 8. Only the relevant levels are displayed. The corresponding decay branches from states of ^{17}C, ^{16}C and ^{15}C with (3p-xh) (x= 0, 1, 2, respectively) neutron configurations to states of (2p-xh) configurations are indicated by the lines connecting the parent states with the daughter states. The ground states of the ^{14}C, ^{15}C and ^{16}C are shifted to the level of the one-neutron thresholds of ^{15}C, ^{16}C and ^{17}C, respectively. Note the strong similarity between the decay pattern of the decays from ^{17}C to ^{16}C and from ^{15}C to ^{14}C.

with the orbital angular momentum ℓ=2, because it has a dominant $(1d5/2)^3$ configuration. The decay to the 0^+ ground state would increase the decay energy. But then a decay orbital angular momentum of ℓ=4 is required and the high centrifugal barrier reduces this decay branch very much. A neutron decay with ℓ=0 to the 4^+_1 state of ^{16}C is forbidden by energy conservation.

The $(11/2^+)$ state in ^{17}C at 7.47 MeV is situated about 1.3 MeV above the *three*-neutron threshold and has an experimental width of Γ_{exp}= 0.5(1) MeV. The decay to the state at 6.11 MeV in ^{16}C, which was assigned tentatively as 3^-, will not fit, because the latter state has a (3p-1h) configuration, as discussed in connection with the 0.31 MeV state in ^{17}C, but a (2p-0h) configuration is needed as final configuration. According to the SM-calculations we assume a $[(1d5/2)^2_{4^+} \otimes (1d3/2)]_{11/2^+}$ configuration for the $11/2^+$ state, and therefore a neutron decay to the ^{16}C 4^+_1 state by the emission of a 1d3/2 or 1d5/2 neutron is most probable. As shown in fig. 8, this decay leads to a particle-stable state of ^{16}C, which prevents further particle decays, although the decay started above the 3n-threshold. The same conditions are met not only for the next lower state of ^{17}C, but for all lower-lying states: already the one-neutron emission leads to states of ^{16}C, which are particle-stable. The one-neutron decay determines the widths, if the decay branches of simultaneous emission of two or three neutrons can be neglected.

Table 8. Decay properties of resonances in ^{17}C (upper part), ^{16}C (central part) and ^{15}C (lower part). For each decay branch the excitation energy $E_{x,i}$, resonance energy E_R and spin-parity J_i^π of the initial state and the excitation energy $E_{x,f}$ and spin-parity J_f^π of the final state is specified. Then the resonance energies E_R^* with respect to *excited* states at $E_{x,f}$ in the daughter nucleus are given according to eq. (6) and the decay scheme of fig. 8. From the measured widths Γ_{exp} (column 9) the reduced widths $\gamma^2_{\ell,exp}$ are calculated according to eq. (8) assuming decay ℓ-values from ℓ=0 to ℓ=3, these results and the relative error in percent are given in the next following five columns. The states are numbered in column 2 in the same way as in table 3, states of the three isotopes with corresponding structure in ^{17}C, ^{16}C and ^{15}C have the same number.

		$E_{x,i}$	E_R	J_i^π	$E_{x,f}$	J_f^π	E_R^*	Γ_{exp}	$\gamma^2_{\ell,exp}$ [MeV]				err.
Decay	No.	[MeV]	[MeV]		[MeV]		[MeV]	[MeV]	ℓ=0	ℓ=1	ℓ=2	ℓ=3	[%]
	2	2.06	1.33	$(\frac{3}{2}^+)$	0.00	0^+	1.33	**0.25**(12)	0.085	0.12	**0.37**	3.06	50
^{17}C	3	**3.10**	2.37	$\frac{9}{2}^+$	1.77	2^+	0.60	**0.08**(4)	0.041	0.08	**0.55**	12.1	50
$\rightarrow^{16}$C	4	4.25	3.52	$(\frac{5}{2}^+,\frac{9}{2}^+)$	1.77	2^+	1.75	**0.14**(7)	0.042	0.06	**0.13**	0.77	50
	5	6.20	5.47	$(\frac{5}{2}^+)$	3.03	0^+	2.44	**0.35**(15)	0.088	0.11	**0.21**	0.80	40
					3.98	2^+	1.49	**0.35**(15)	0.113	0.16	**0.43**	3.06	40
	6	7.47	6.74	$(\frac{11}{2}^+)$	4.14	4^+	2.60	**0.58**(10)	0.122	0.15	**0.31**	1.00	20
	2	7.74	3.49	$(1^-$- $3^-)$	3.10	$\frac{1}{2}^-$	0.39	**0.15**(4)	0.094	0.24	2.69	97.0	20
^{16}C	3	**8.92**	4.67	5^-	4.22	$\frac{3}{2}^-$	0.45	**0.04**(2)	0.023	0.06	**0.52**	160	50
$\rightarrow^{15}$C	4	9.98	5.73	$(3^-,5^-)$	4.22	$\frac{5}{2}^-$	1.51	**0.12**(3)	0.038	0.05	**0.14**	1.02	25
				(3^-)	4.66	$\frac{7}{2}^-$	1.07	**0.12**(3)	0.046	0.07	**0.26**	2.88	25
	5	11.85	7.60	(3^-)	5.87	$\frac{7}{2}^-$	1.73	**0.22**(4)	0.066	0.09	**0.21**	1.27	20
	–	12.54	8.29	(3^-)	5.87	$\frac{5}{2}^-$	2.42	(**0.2**(1))	0.051	0.06	**0.12**	0.47	50
					6.84	$\frac{5}{2}^-$	1.45	(**0.2**(1))	0.065	0.09	**0.26**	1.92	50
	6	13.12	8.87	$(6^-,5^-)$	6.84	$\frac{5}{2}^-$	2.03	**0.40**(10)	0.110	0.14	**0.30**	1.48	25
	2	8.45	7.23	$(\frac{3}{2}^+)$	6.59	0^+	0.64	**0.040**(15)[a]	0.019	0.04	**0.24**	4.80	50
^{15}C	3	**9.75**	8.53	$(\frac{9}{2}^+)$	8.32	2^+	0.21	**0.020**(15)[a]	0.013	0.05	**1.03**	69.0	70
$\rightarrow^{14}$C	4	11.05	9.83	$(\frac{5}{2}^+,\frac{9}{2}^+)$	8.32	2^+	1.51	**0.10**(5)	0.032	0.05	**0.12**	0.86	50
	5	13.1	11.88	$(\frac{5}{2}^+)$	9.75	0^+	2.13	**0.30**(8)	0.081	0.11	**0.22**	1.00	30
					10.43	2^+	1.45	**0.30**(8)	0.098	0.14	**0.39**	2.91	30
	–	13.8	12.58	$(\frac{5}{2}^+,\frac{7}{2}^+)$	10.43	2^+	2.15	(**0.3**(2))	0.081	0.10	**0.21**	0.97	67
	6	14.57	13.35	$(\frac{11}{2}^+)$	11.73	4^+	1.62	**0.13**(5)	0.040	0.06	**0.14**	0.92	40
					10.74	4^+	2.61	0.13(5)	0.032	0.04	0.07	0.26	40

[a] [34,35]

We have calculated from the widths Γ_{exp}, which were obtained from the analysis of the spectra, the experimental values of reduced widths $\gamma^2_{\ell,exp}$ according to eq. (8) for the one-neutron decay from states of ^{17}C to ^{16}C, from ^{16}C to ^{15}C and also from ^{15}C to ^{14}C (see upper, central and lower part of table 8, respectively).

$$\gamma^2_{\ell,exp} = \frac{\Gamma_{exp}}{2\ P_\ell(E^*_{dec}(J_i^\pi, J_f^\pi))} \qquad (8)$$

The dependence of the decay energy E^*_{dec} on both excited states according to eq. (7) is indicated explicitly in eq. (8). One can see, that the ℓ-dependence of the reduced width $\gamma^2_{\ell,exp}$ results only from the ℓ-dependence of the penetrability $P_\ell(E_{dec})$. The penetrabilities are calculated at a channel radius of 6 fm (as before) using the decay energies at resonance E^*_R given in table 8, column 8.

The reduced width $\gamma^2_{\ell,exp}$ represents the physical quantity of interest for structure information. The values obtained for ℓ=2 decays from ^{17}C states range from 0.13 to 0.55 in good agreement with expectations, whereas those for ℓ= 0 are very small. Assuming ℓ= 1 for the neutron decays results also in rather small values, but anyway, (1p) shell configurations are most probably not populated in ^{17}C in the present reaction, as discussed above. The values of the reduced widths for decays of ^{17}C with ℓ= 3 are fluctuating strongly (table 8) due to the stronger sensitivity of the penetrability at these low decay energies to the higher centrifugal barrier. For this reason the values of $\gamma^2_{\ell=3,exp}$ are not very reliable, although in some cases decays with ℓ= 3 might not be completely excluded. But further arguments from the general systematics and the SM-calculations support definitely a preference for decay angular momenta of ℓ= 2. The values for decays with ℓ= 4 (not shown in table 8) are always by far too large, they are an order of magnitude larger than the ones for ℓ= 3.

The calculations for the decay of ^{16}C states have been performed in the same way as for ^{17}C. Here we consider the neutron decay of (3p-1h) structures to states of ^{15}C with a (2p-1h) structure (fig. 8). The reduced widths show a similar good agreement for ℓ= 2 decays, except for the 7.74 MeV state, where the reduced width is too large by at least a factor of five. This is obviously related to the steep energy dependence of the penetrability near the threshold. The decay energy at resonance, E^*_R, has a value of only 0.39 MeV for this state. The larger width Γ_{exp} may be explained assuming contributions also from an ℓ= 0 (2s1/2) decay component in the wave function in addition to ℓ= 2.

The next state at 8.92 MeV has a similar small value of the decay energy E^*_R= 0.45 MeV, but also Γ_{exp} is small (table 8). Here we assumed a stretched $(1d5/2)^3_{9/2^+}$ neu-

tron configuration according to the structure of the corresponding state in ^{17}C and therefore expect an almost pure $\ell = 2$ decay. The experimental value of the reduced width $\gamma^2_{\ell=2,exp} = 0.52$ MeV is in very good agreement with the expectations in this case.

All the (3p-2h) resonances of ^{15}C analyzed in this measurement have very similar values for the reduced widths as compared to the corresponding (3p-0h) resonances in ^{17}C. This result shows that the decays from the (1d) neutron orbits are the dominant components in most cases, and it confirms the similar structure of these states for ^{15}C and ^{17}C.

5 Conclusions

Excited states of ^{17}C above the neutron threshold have been observed up to 16.3(1) MeV excitation energy using the (^{12}C,^{9}C) three-neutron transfer reaction on ^{14}C. These are compared to states of ^{16}C and ^{15}C obtained in the same reaction on ^{13}C and ^{12}C targets. The incident energy in all cases is 19.2 MeV/u. The large negative ground state Q-values of about -40 MeV and the dynamical reaction conditions impose strong and selective matching conditions for the population of final states. In this reaction preferentially neutron (sd)^3 structures are populated.

A comparison of the level schemes of ^{17}C and ^{16}C shows the surprising result, that the excitation energies of almost all states observed in ^{17}C agree with excitation energies in ^{16}C [27] within variations of the differences of only -0.17/+0.23 MeV, when a constant offset of 5.82 MeV is taken into account. The situation is similar for ^{15}C states populated in the three-neutron transfer, where the variations are somewhat larger, and the mean offset is 6.85 MeV.

Most of these states are particle-unstable and therefore are described as Breit-Wigner resonances. Also the widths of the corresponding states and the relative cross sections show a similar regular behaviour as the excitation energies. These results can be well understood in the weak coupling model: the transferred neutrons are placed into (sd)^3 configurations and the target nuclei become the cores of the structures, in accordance with the population mechanism of a direct three-neutron transfer. These structures are confirmed by SM-calculations and also by comparison to states of ^{19}O with corresponding structure.

Decay schemes of the neutron decays from states with (3p-xh) configurations in ^{17}C (x=0), ^{16}C (x=1), and ^{15}C (x=2) to states of ^{16}C, ^{15}C, ^{14}C with known (2p-xh) configurations [24–27,32] have been proposed (fig. 8). The decay energies from the parent to the corresponding daughter states are in this case much smaller than for the decay to the ground state of the daughter nucleus. Using these decay energies in the calculation of the penetrabilities for the neutron decays, experimental values of reduced widths have been obtained from the measured width parameters. The calculations have been performed for a variety of decay ℓ-values to show its sensitivity on the decay angular momentum ℓ. For ^{17}C in almost all cases the best agreement with expected values for the reduced widths, which are in the range between 0.1 MeV and 0.6 MeV, is obtained for $\ell = 2$ decays, which confirms the dominant population of 1d-configurations in ^{17}C. Small admixtures of $\ell = 0$ contributions have to be assumed in some cases. Very similar results are obtained also for the corresponding states of ^{16}C and ^{15}C.

6 Acknowledgements

The authors thank the ISL accelerator staff for the stable operation of the cyclotron. The precise ERDA measurement of the ^{14}C-target composition by Drs. W. Bohne, J. Röhrich and E. Strub from ISL (HMI) is gratefully acknowledged. G. de A. and C. W. are grateful to the Alexander-von-Humboldt Foundation for support.

References

1. D. Bazin, W. Benenson, B. A. Brown, J. Brown, B. Davids, M. Fauerbach, P. G. Hansen, P. Mantica, D. J. Morrissey, C. F. Powell, B. M. Sherrill, and M. Steiner, Phys. Rev. C **57**, 2156 (1998).
2. T. Baumann, M. J. G. Borge, H. Geissel, H. Lenske, K. Markenroth, W. Schwab, M. H. Smedberg, T. Aumann, L. Axelsson, U. Bergmann, D. Cortina-Gil, L. Fraile, M. Hellström, M. Ivanov, N. Iwasa, R. Janik, B. Jonson, G. Münzenberg, F. Nickel, T. Nilsson, A. Ozawa, A. Richter, K. Riisager, C. Scheidenberger, G. Schrieder, H. Simon, B. Sitar, P. Strmen, K. Sümmerer, T. Suzuki, M. Winkler, H. Wollnik, M. V. Zhukov, Phys. Lett. B **439**, 256 (1998).
3. D. Cortina-Gil, T. Baumann, H. Geissel, H. Lenske, K. Sümmerer, L. Axelsson, U. Bergmann, M. J. G. Borge, L. Fraile, M. Hellström, M. Ivanov, N. Iwasa, R. Janik, B. Jonson, K. Markenroth, G. Münzenberg, F. Nickel, T. Nilsson, A. Ozawa, K. Riisager, G. Schrieder, W. Schwab, H. Simon, C. Scheidenberger, B. Sitar, T. Suzuki, and M. Winkler, Eur. Phys. J. A **10**, 49 (2001).
4. E. Sauvan, F. Carstoiu, N. A. Orr, J. S. Winfield, M. Freer, J. C. Angélique, W. N. Catford, N. M. Clarke, M. Mac Cormick, N. Curtis, S. Grévy, C. Le Brun, M. Lewitowicz, E. Liégard, F. M. Marqués, P. Roussel-Chomaz, M.-G. Saint Laurent, and M. Shawcross, Phys. Rev. C **69**, 044603 (2004).
5. C. Wu, Y. Yamaguchi, A. Ozawa, R. Kanungo, I. Tanihata, T. Suzuki, D. Q. Fang, T. Suda, T. Ohnishi, M. Fukuda, N. Iwasa, T. Ohtsubo, T. Izumikawa, R. Koyama, W. Shinozaki, M. Takahashi, Nucl. Phys. A **739**, 3 (2004).
6. V. Maddalena, T. Aumann, D. Bazin, B. A. Brown, J. A. Caggiano, B. Davids, T. Glasmacher, P. G. Hansen, R. W. Ibbotson, A. Navin, B. V. Pritychenko, H. Scheit, B. M. Sherrill, M. Steiner, J. A. Tostevin, and J. Yurkon, Phys. Rev. C **63**, 024613 (2001).
7. U. Datta Pramanik, T. Aumann, K. Boretzki, B. V. Carlson, D. Cortina, Th. W. Elze, H. Emling, H. Geissel, A. Grünschloss, M. Hellström, S. Ilievski, J. V. Kratz, R. Kulessa, Y. Leifels, A. Leistenschneider, E. Lubkiewicz, G. Münzenberg, P. Reiter, H. Simon, K. Sümmerer, E. Wajda, W. Walus, Phys. Lett. B **551**, 63 (2003).

8. D. Ridikas, M. H. Smedberg, J. S. Vaagen, M. V. Zhukov, Nucl. Phys. A **628**, 363 (1998).
9. Hiroyuki Sagawa, Toshio Suzuki, Kouichi Hagino, Nucl. Phys. A **722**, 183c (2003).
10. Toshio Suzuki, Hiroyuki Sagawa, Kouichi Hagino, Phys. Rev. C **68**, 014317 (2003).
11. P. Descouvemont, Nucl. Phys. A **675**, 559 (2000).
12. E. K. Warburton and B. A. Brown, Phys. Rev. C **46**, 923 (1992).
13. D. J. Millener and D. Kurath, Nucl. Phys. **255**, 315 (1975).
14. J. A. Nolen, T. S. Bhatia, H. Hafner, P. Doll, C. A. Wiedner and G. Wagner, Phys. Lett. **71B**, 314 (1977).
15. L. K. Fifield, J. L. Durell, M. A. C. Hotchkis, J. R. Leigh, T. R. Ophel, and D. C. Weisser, Nucl. Phys. A **385**, 505 (1982).
16. E. K. Warburton and D. J. Millener, Phys. Rev. C **39**, 1120 (1989).
17. J. P. Dufour, R. Del Moral, A. Fleury, F. Hubert, D. Jean, M. S. Pravikoff, H. Delagrange, H. Geissel, and K.-H. Schmidt, Z. Phys. A **324**, 487 (1986).
18. M. S. Curtin, L. H. Harwood, J. A. Nolen, B. Sherrill, Z. Q. Xie, and B. A. Brown, Phys. Rev. Lett. **56**, 34 (1986).
19. H. Ogawa, K. Asahi, H. Ueno, K. Sakai, H. Miyoshi, D. Kameda, T. Suzuki, H. Izumi, N. Imai, Y. X. Watanabe, K. Yoneda, N. Fukuda, H. Watanabe, A. Yoshimi, W. Sato, N. Aoi, M. Nagakura, T. Suga, K. Yogo, A. Goto, T. Honda, Y. Kobayashi, W.-D. Schmitt-Ott, G. Neyens, S. Teughels, A. Yoshida, T. Kubo, and M. Ishihara, Eur. Phys. J. A **13**, 81 (2002).
20. M. Stanoiu, F. Azaiez, F. Becker, M. Belleguic, C. Borcea, C. Bourgeois, B. A. Brown, Z. Dlouhý, Z. Dombrádi, Z. Fülöp, H. Grawe, S. Grévy, F. Ibrahim, A. Kerek, A. Krasnahorkay, M. Lewitowicz, S. Lukyanov, H. van der Marel, P. Mayet, J. Mrázek, S. Mandal, D. Guillemaud-Mueller, F. Negoita, Y. E. Penionzhkevich, Z. Podolyák, P. Roussel-Chomaz, M. G. Saint Laurent, H. Savajols, O. Sorlin, G. Sletten, D. Sohler, J. Timár, C. Timis, and A. Yamamoto, Eur. Phys. J. A **20**, 95 (2004).
21. Z. Elekes, Zs. Dombrádi, R. Kanungo, H. Baba, Zs. Fülöp, J. Gibelin, Á. Horváth, E. Ideguchi, Y. Ichikawa, N. Iwasaki, S. Kanno, S. Kawai, Y. Kondo, T. Motobayashi, M. Notani, T. Onishi, A. Ozawa, H. Sakurai, S. Shimoura, E. Takeshita, S. Takeuchi, I. Tanihata, Y. Togano, C. Wu, Y. Yamaguchi, Y. Yanagisawa, A. Yoshida, and K. Yoshida, Phys. Lett. B **614**, 174 (2005).
22. G. Raimann, A. Ozawa, R. N. Boyd, F. R. Chloupek, M. Fujimaki, K. Kimura, T. Kobayashi, J. J. Kolata, S. Kubono, I. Tanihata, Y. Watanabe, and K. Yoshida, Phys. Rev. C **53**, 453 (1996).
23. D. P. Balamuth, J. M. Lind, K. C. Young, Jr., and R. W. Zurmühle, Nucl. Phys. **A290**, 65 (1977).
24. H. T. Fortune, R. Middleton, M. E. Cobern, G. E. Moore, S. Mordechai, R. V. Kollarits, H. Nann, W. Chung, and B. H. Wildenthal, Phys. Lett. **70B**, 408 (1977).
25. H. T. Fortune, M. E. Cobern, S. Mordechai, G. E. Moore, S. Lafrance, and R. Middleton, Phys. Rev. Lett. **40**, 1236 (1978).
26. R. R. Sercely, R. J. Peterson and E. R. Flynn, Phys. Rev. C **17**, 1919 (1978).
27. H. G. Bohlen, R. Kalpakchieva, B. Gebauer, S. M. Grimes, H. Lenske, K. P. Lieb, T. N. Massey, M. Milin, W. von Oertzen, Ch. Schulz, T. Kokalova, S. Torilov, and S. Thummerer, Phys. Rev. C **68**, 054606 (2003).
28. A. G. Drentje, H. A. Enge and S. B. Kowalski, Nucl. Instr. Meth. **122**, 485 (1974).
29. H. G. Bohlen, R. Kalpakchieva, A. Blažević, B. Gebauer, T. N. Massey, W. von Oertzen, and S. Thummerer, Phys. Rev. C **64**, 024312 (2001).
30. A.M. Lane and R.G. Thomas, Rev. Mod. Phys. **30**, 257 (1958).
31. D. M. Brink, Phys. Lett. **40B**, 37 (1972).
32. W. von Oertzen, H. G. Bohlen, M. Milin, Tz. Kokalova, S. Thummerer, A. Tumino, R. Kalpakchieva, T. N. Massey, Y. Eisermann, G. Graw, T. Faestermann, R. Hertenberger and H.-F. Wirth, Eur. Phys. J. A **21**, 193 (2004).
33. I. P. Thompson, Computer Phys. Reports **7**, 167 (1988).
34. F. Ajzenberg-Selove, Nucl. Phys. **A523**, 1 (1991) and F. Ajzenberg-Selove, Nucl. Phys. **A360**, 1 (1981).
35. J. D. Garrett, F. Ajzenberg-Selove and H. G. Bingham, Phys. Rev. C **10**, 1730 (1974).
36. S. Truong and H. T. Fortune, Phys. Rev. C **28**, 977 (1983).
37. G. Murillo, S. Sen and S. E. Darden, Nucl. Phys. **A579**, 125 (1994).
38. S. E. Darden, G. Murillo and S. Sen, Phys. Rev. C **32**, 1764 (1985).
39. H. G. Bohlen, R. Kalpakchieva, W. von Oertzen, T. N. Massey, B. Gebauer, Tz. Kokalova, A. A. Ogloblin, Ch. Schulz, and S. Thummerer, Nucl. Phys. **A738**, 333 (2004).
40. H. G. Bohlen, R. Kalpakchieva, W. von Oertzen, T. N. Massey, A. A. Ogloblin, G. de Angelis, Tz. Kokalova, Ch. Schulz, and C. Wheldon, J. Phys. G **31**, S1461 (2005).
41. F. E. Cecil, J. R. Shepard, R. E. Anderson, R. J. Peterson and P. Kaczkowski, Nucl. Phys. **A255**, 243 (1975).
42. S. E. Darden, S. Sen, H. R. Hiddleston, J. A. Aymar and W. A. Yoh, Nucl. Phys. **A208**, 77 (1973).
43. H. Ohnuma, N. Hoshino, O. Mikoshiba, K. Raywood, A. Sakaguchi, G. G. Shute, B. M. Spicer, M. H. Tanaka, M. Tanifuji, T. Terasawa and M. Yasue, Nucl. Phys. **A448**, 205 (1985).
44. D. J. Millener, D. I. Sober, H. Crannell, J. T. O'Brien, L. W. Fagg, S. Kowalski, C. F. Williamson, L. Lapikas, Phys. Rev. C **39**, 14 (1989).
45. F. Delaunay, F. M. Nunes, W. G. Lynch, and M. B. Tsang, Phys. Rev. C **72**, 014610 (2005).
46. E. Stiliaris, H. G. Bohlen, X. S. Chen, B. Gebauer, A. Miczaika, W. von Oertzen, W. Weller and T. Wilpert, Z. Phys. A. **326**, 139 (1987).
47. W. Rae, A. Etchegoyen, B. A. Brown, OXBASH, The Oxford-Buenos Aires-MSU shell-model code, Tech. Rep. 524, Michigan State University Cycl. Lab., 1985
48. D. R. Tilley, H. R. Weller, C. M. Cheves and R. M. Chasteler, Nucl. Phys. **A595**, 1 (1995).
49. E. K. Warburton, Phys. Rev. C **38**, 935 (1988), and refs. therein.
50. H. T. Fortune and H. G. Bingham, Nucl. Phys. **A293**, 197 (1977).
51. C. B. Fulmer, G. R. Satchler, K. A. Erb, D. C. Hensley, R. L. Auble, J. R. Ball, F. E. Bertrand and E. E. Gross, Nucl. Phys. **A427**, 545 (1984).
52. S. Cohen and D. Kurath, Nucl. Phys. **A101**, 1 (1967).